TÉCNICO LISBOA

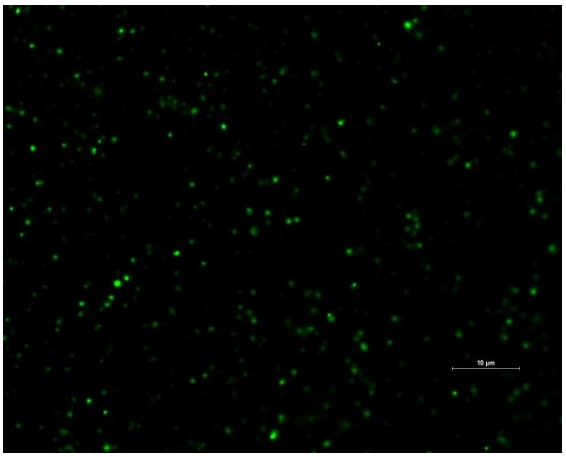

Hybrid Nano-biocomposites for skin care applications

Henrique Palma da Silva

Thesis to obtain the Master of Science Degree in

Biological Engineering

Supervisors: Prof. Tzanko Tzanov/Prof. Frederico Castelo Alves Ferreira

Examination Committee

Chairperson: Prof. Jorge Humberto Gomes Leitão

Supervisor: Prof. Frederico Castelo Alves Ferreira

Member of the Committee: Prof. Carlos Miguel Calisto Baleizão

October of 2016

ACKNOWLEDGEMENTS

I would like to thank Professor Tzanko Tzanov for receiving me and being my supervisor during my internship at the Molecular and Industrial Biotechnology Group (GBMI) of Universitat Politècnica de Catalunya (UPC) in Terrassa, allowing me to experience the daily life of an investigator and grow both personally and academically. I'm grateful to everyone at the GBMI for welcoming me with open arms as their colleague, providing a fun working environment while still being very hardworking people. A special thanks to Dr. Eva Ramón and Ph.D. student Kristina Ivanova which gave me the guidance, scientific knowledge and support throughout my work. I would also like to thank Prof. Frederico Ferreira for being my supervisor at Instituto Superior Técnico (IST). A big thanks to all of my friends that accompanied me not only in the period of my work in UPC, but also during the last 5 years of my graduation, always supporting and bringing happiness to my daily life. Lastly, and most importantly, I'm very grateful to my parents and sister, which made an effort for me to have the best international experience possible, while giving me constant support throughout all of it, without them, none of this could have happened.

Thank you!

RESUMO

Esta tese procura servir de base para o desenvolvimento de novos e alternativos materiais antibacterianos de forma a combater o desenvolvimento de resistência, nomeadamente, a antibióticos, por parte das bactérias causadoras de infecções na pele. Para isso está dividida em duas secções. Primeiramente, o revestimento da superficie de nanoparticulas (NP) de Gantrez comercial através da técnica de "layer-by-layer" (LbL) com adição successiva de polielectrólitos de cargas opostas, especificamente, a aminocelulose e o ácido hialurónico. A aminocelulose, para além de ter propriedades antibacterianas, possui grupos funcionais que permitirão a ligação de moléculas de "quorum sensing", que permitirão "cell targetting". Em segundo, a optimização do protocolo de produção e purificação de uma enzima de "quorum quenching", a lactonase, que futuramente será incorporada nas partículas LbL, melhorando o efeito antibacteriano. Para produzir as NPs LBL, as particulas de Gantrez foram diluidas separadamente até $1.98x10^{12}$NP/ml, $9.9x10^{11}$NP/ml e $4.95x10^{11}$ NP/ml, e, após cada deposição de polielectrólito, a purificação das mesmas foi feita através de ultracentrifugação, obtendo-se partículas com 5 camadas e tamanhos médios, medidos através de NTA, de 401nm, 302nm e 369nm, respectivamente, e 665nm, 717nm e 726nm, respectivamente, através de DLS. Os valores de PDI finais foram 0.424, 0.864 e 0.771, respectivamente, obtendo-se também, rendimentos de purificação de 1.14%, 1.21% e 0.624%, respectivamente. Quanto à produção e purificação de lactonase, a proteína foi produzida com sucesso, e foi possível aferir, através de coloração com Coomassie e Western Blot, que a proteína elui a concentrações de imidazole em tampão HNa_2PO_4/H_2NaPO_4 maiores ou iguais a 250mM.

PALAVRAS-CHAVE: Antibacteriano; Nanopartículas; Polielectrólitos; Layer-by-Layer; Lactonase.

ABSTRACT

Skin and soft tissues infections (SSTIs) treatment is based majorly in the use of antibiotics, but the recent rise in microbial drug resistance is a growing challenge for future therapies of bacterial infections. This thesis seeks to be the base to the development of new and alternative antibacterial materials, specifically, for SSTIs. To accomplish that, it is divided in two separate sections. Firstly, successive depositions of oppositely charged polyelectrolyte layers (PE) allowing the coating of commercially available Gantrez nanoparticles (NP) with layer-by-layer (LbL) technique. The use of aminocellulose, besides providing antibacterial effect, introduces functional moieties for further grafting of quorum sensing (QS) molecules that will allow directed cell targeting. Secondly, the optimization of the production and purification protocol of the quorum quenching enzyme lactonase, which in the future will be incorporated in the LbL particles, enhancing antibacterial effect. For LbL NPs production, the Gantrez NPs dilutions were $1.98x10^{12}$NP/ml, $9.9x10^{11}$NP/ml and $4.95x10^{11}$ NP/ml. Purification, after each PE deposition, was made through ultracentrifugation, resulting in particles with 5 layers, with a mean size of 401nm, 302nm and 369nm, respectively, measured through NTA and 665nm, 717nm and 726nm, respectively, measured through DLS. At the same time, their final PDI was 0.424, 0.864 and 0.771, respectively. The final purification yields were 1.14%, 1.21% and 0.624%, respectively. Regarding the production and purification of lactonase, the protein was produced and assessed through Coomassie staining and Western Blot that, in the purification step, the protein elutes at values higher than 250mM of Imidazole concentration in HNa_2PO_4/H_2NaPO_4 buffer.

KEYWORDS: Antibacterial; Nanoparticles; Polyelectrolyte; Layer-by-Layer; Lactonase

CONTENTS

LIST OF FIGURES

LIST OF TABLES

LIST OF ABRREVIATIONS

ε	Dielectric Constant
$	American dollars
AC	6-deoxy-6-(w-aminoalkyl) amino-cellulose
ACP	Acyl carrier protein
AHL	Acyl homoserine lactone
AI	Autoinducers
AIP	Autoinducing peptides
ANP	Antibacterial Nanoparticle
APS	Ammonium Persulfate
bp	base pairs
D	Translational diffusion coefficient
d(H)	Hydrodynamic diameter
Da	Dalton
DLS	Dynamic Light Scattering
DMSO	Dimethyl Sulfoxide
DNA	DeoxyriboNucleic Acid
DTT	1,4-Dithiothreitol
EB	Ethidium Bromide
EDTA	Ethylenediaminetetraacetic acid
EU	European Union
f(ka)	Henry's function
FITC	Fluoroscein Isothiocyanate
FT	Flow-Through
GBMI	Molecular and Industrial Biotechnology Group
HA	Hyaluronic Acid
HABI	Hospital-acquired bacterial infections
HK	Histidine kinase
HRP	Horseradish Peroxidase
IPTG	Isopropyl β-D-1-thiogalactopyranoside
k	Boltzmann's constant
LB	Luria Bertani
LbL	Layer-by-Layer
MD	Matrix-Degrading
MDR	Multidrug-resistant
MH	Mueller Hinton
MPO	Myeloperoxidase
mQ	milliQ
Mw	Molecular weigth
NADPH	Nicotamine Adenine Dinucleotide Phosphate
NP	Nanoparticle
NTA	Nanoparticle Tracking Analysis
OD	Optical Density

PAGE	Polyacrylamide gel electrophoresis
PDI	Polidispersity Index
PE	Polyelectrolyte
PMSF	Phenylmethylsulfonyl Fluoride
QPEI	Polycationic Nanoparticle
QQ	Quorum Quenching
QS	Quorum Sensing
RNA	Ribonucleic Acid
RNS	Radical Nytrogen Species
ROS	Radical Oxygen Species
SAM	S-adenosylmethionine
SDS	Sodium Dodecyl Sulfate
SKINCHAPS	SKin Healthcare by Innovative NanoCAPsuleS
SSTI	Skin and soft tissue infections
T	Absolute temperature
TAE	Tris-acetate-EDTA buffer
TBS	Tris-buffered saline buffer
TEMED	N,N,N',N'-tetramethylethane-1,2-diamine
U_E	Electrophoretic Mobility
USA	United States of America
UV	Ultraviolet
ZP/ ζ	Zeta Potential
η	Viscosity

1 Introduction

The work developed in this thesis was inserted in a European project called SKHINCAPS (SKin Healthcare by Innovative NanoCAPsuleS). This project has as main objective, the development of the know-how and process to manufacture, sustainable safe, cost-effective and highly stable nanocapsules with different encapsulated active principles for incorporation in skin care products, such as lotions, creams and textiles. The novel nanocapsules will be used in 3 different applications: skin thermal comfort, anti-ageing and anti-microbial infections.

This thesis focus was to serve as the basis to the development of novel nanocapsules for skin applications that have an enhanced antimicrobial effect, that doesn't help bacteria to develop resistance. The main barrier against microbial invasion is the skin, as it is constantly in contact with the external environment and several microorganisms are able to colonize it. The vast majority of the colonizing flora consists of bacteria, both gram-positive and gram-negative species. The skin, besides being a physical barrier to these organisms, has other defense mechanisms. Secretion of low pH, sebaceous fluid and fatty acids can inhibit the growth of pathogens and its natural micro flora, deters other microbial colonization. But, if the bacteria penetrate the integumentary barrier, they can damage the tissue and generate an inflammatory response[1].

The estimated incidence rate of these infections is 24.6 per 1000 person per year, approximately 7% to 10% of the total of hospitalized patients are affected by skin and soft tissue infections (SSITs), and among the patients with infection only, in the emergency care setting, SSITs represent the third most common diagnosis, after only chest pain and asthma[1]. SSTIs treatment is traditionally a pharmacotherapeutic approach based on antibiotics, which doesn't provide a sustainable solution. With increased antibiotic exposure and prolonged hospitalization, patients are at an increased risk of infections by antibiotic resistant species[1].

Not only SSTIs are suffering with the appearance of these species. Ever since the mass production of penicillin in the 1940's started, up until the 70's, a large amount of new antibiotics was found, giving birth to what is known today as the golden era of discovery of novel antibiotics classes, and, with the decline of the discovery rate, modifications of the known antibiotics emerged[2]. Unfortunately, due to the overuse of these drugs, bacteria started to develop antibiotic resistance, and multidrug-resistant (MDR) bacteria strains started to appear. Infections caused by these bacteria kill 25,000 patients in the EU each year [3] and more than 63,000 in the US, from hospital-acquired bacterial infections(HABI) [4]. Economic wise, extra healthcare costs and productivity losses account for 1.5 billion € (in 2009 euros) each year in the EU[3], while on the US, the additional cost of treating HABIs from just six species of MDR bacteria was estimated to be $1.87 billion (in 2006 dollars)[4].

Bacteria resistance happens mainly for two reasons. On one hand, bacteria (and other microorganisms) are able to develop antibiotic resistance due to natural selection[5]. On the other hand, bacteria have a mechanism called “conjugation”, where a bacteria that has developed resistance against an antibiotic, can transfer the genes responsible for that resistance to other bacteria, usually through a plasmid (circular small piece of DNA that is sized 1-200Kbps), spreading the resistance throughout the population[6]. This mechanism is regulated through another mechanism that allows bacteria to regulate gene expression in response to fluctuations in cell-population density, named Quorum Sensing (QS). QS bacteria produce and release chemical signaling molecules called autoinducers (AI’s) that increase proportionally to cell density. When a minimum concentration of AI’s is detected, certain genes have a modification of expression, allowing regulation of several processes, including the mentioned conjugation[7].

Conventional antibiotics kill or interfere with essential housekeeping functions like DNA, RNA and protein synthesis. This imposes a life-or-death selection pressure, promoting evolution of the resistance in these microorganisms. This shows the importance of finding new treatments for bacteria related diseases, which, preferably, do not help bacteria develop new forms of resistance. In recent years, alternative methods have been explored, and the most promising strategies are Quorum Quenching and Antibacterial Nanoparticles, which are the basis of this thesis.

QQ is known as signal interference, blocking cell-to-cell communication, disabling the activation of the genes that allow regulation of bacterial processes that are quorum sensing dependent[8].As QQ doesn’t interfere with housekeeping functions of bacteria, it is a promising new antibacterial strategy with lower risk (resistance development wise) than conventional antibiotics. A few enzymes have been proved to degrade QS signaling AIs, like the AHL-lactonase and AHL-acylase, resulting in low virulence without enhancing antibiotic-resistance[9].

With the discovery of these molecules, new techniques based on immobilization for covalent grafting and Layer-by-Layer (LbL) coatings have emerged as antimicrobial strategies. A previous study of grafting of cellobiose dehydrogenase in polydimethylsiloxane in urinary catheters coatings showed an effective reduction of viable bacteria cells and biofilm formation under both static and dynamic conditions by 60 and 70%, respectively[10]. In our laboratory, another study, where a hybrid system with QQ enzymes and matrix-degrading enzymes in a multilayer coating in urinary catheters has shown significant capacity (up to 70%) of degrading QS signaling molecules and polysaccharide components of the biofilm matrix, making them potentially applicable as antibiofilm agents when applied to these coatings, having an increased inhibiting power, more so then when applied by themselves[11].

Antibacterial Nanoparticles are not a part of the QQ methods, but have also been proven to be an efficient antibacterial approach that doesn’t develop resistance. These can be grouped in organic or inorganic particles, where the inorganic are majorly metal based, while the organic are polymer based and both of these materials have antimicrobial effect[12], [13]. These materials do not develop

resistance because of the vast range of antibacterial mechanisms inherent to them [14]. When these materials are coupled with nanoparticles, their effect is enhanced.

1.1 Objectives

This thesis aims to mix both the QQ effect and the Antibacterial Nanoparticles in one single material. For that, the objective was to coat the rather inert surface of commercially available Gantrez nanocaposules with layer by layer technique and introduce functional moieties for further grafting of quorum sensing (QS) molecules. QS molecules may serve as a target for driving with high specificity the antibacterial-loaded nanocapsules to the site of infection,

In this line, the empty capsules were coated with oppositely charged polyelectrolytes – hyaluronic acid and aminocellulose. Based on previous antimicrobial work made in the GBMI, the presence of aminocellulose in the assemblies would not only result in capsules functionalization with amino functional groups but also may impart antibacterial properties against bacteria[15].

This allows the LbL system to go one step ahead, creating an LbL system that, instead of being film based, they would be nanoparticle(NP) based. Meaning, each particle, on their own, had several polyelectrolyte (PE) depositions allowing the creation of an effective and controlled drug-delivery system. Being a PE based system, the QQ enzymes (e.g. acylase and lactonase) and other antibacterial enzymes might be also deposited in the particles shell to synergistically improve the antibacterial/antibiofilm effect towards bacteria. The LbL coated Nanoparticles would allow that the applicability of LbL methods had an increased range, allowing their use in other ways than coatings, like creams, lotions or liquids.

The work made was divided in two different sections. On one hand, the creation and optimization of a reproducible method of LbL NP production based on PE deposition while following the mean size variation, zeta potencial (ZP) and Polydispersity Index (PDI) with each layer deposition. On the other hand, the production of a QQ enzyme (lactonase) and optimization of its production and purification protocol. The purpose of the production of this molecule was its posterior incorporation in the LbL NPs.

1.2 Thesis Structure

This work is arranged in five chapters. Chapter 2 is subdivided in 4 subchapters which give an insight on what are Quorum Sensing and Quorum Quenching and how they work for either gram-negative or gram-positive bacteria. After that, it is described how nanotechnology helps in the development of antimicrobial components in the late years. In chapter 3, the materials and methods used for the Layer-by-Layer Nanoparticles production and lactonase production and purification are described along with some theoretical concepts which allow a higher comprehension on why the experiments where made that way. Chapter 4 discusses and shows the results obtained as well as conclusions on these. Finally, chapter 5 presents the future works based on what was made.

2 State-of-the-art

2.1 Skin and soft tissue infections (SSTIs)

SSTIs are microbiological infections resulted from invasion of the skin and underlying soft tissues by microbial. As the skin is always in contact with the external environment, a large number and variety of organisms exist in this tissue which may produce infections[1]. Besides, the microbial variety existing on each person varies, due to several exogenous and endogenous factors, as shown in **Figure 2.1**[16].

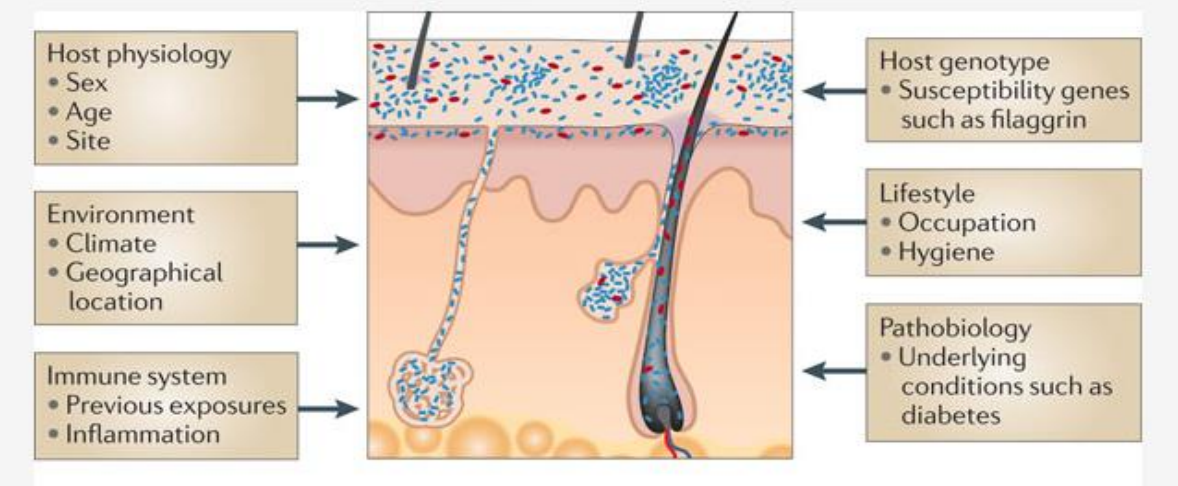

Figure 2.1: Exogenous and Endogenous factors which affect the microbial ecology of the skin, making it unique for each person. Addapted from [16]

The bacterial infection mechanism in the skin depends on three major steps, which are: Bacterial adherence to host cells (skin cells), invasion of the tissue with evasion of the host cells and production of toxins. Virulence genes, in most pathogenic bacteria, encode special proteins that confer these properties[1]. These genes are activated through Quorum-Sensing, which will be explained in detail in the subchapter 2.2.

SSITs are a very relevant medical issue. Depending on a patient's comorbidities, a mild infection can easily and rapidly transform to a life threatening situation. The estimated incidence rate of these infections is 24.6 per 1000 person per year, approximately 7% to 10% of the total of hospitalized patients are affected by SSITs, and among the patients with infection only, in the emergency care setting, SSITs represent the third most common diagnosis, after only chest pain and asthma[1].

Because a large variety of organisms inhabit the skin, not only it makes the diagnosis harder, but also, a unique antimicrobial treatment for every species is impossible to attain nowadays.

After diagnosis, the most conventional treatment used is the prescription of antibiotics, which bring several problems. As resistant microorganisms start to emerge, antibiotics lose their efficiency and new alternative antibacterial methods that do not help bacteria in developing resistance need to appear.

These methods would be based on Quorum Quenching and Nanotechnology, which will be explained in detail in Chapter2.3 and 2.4.

2.2 Quorum Sensing – Bacteria Communication

Quorum sensing is a bacterial cell-to-cell communication process that allows bacteria to share information about cell density and adjust gene expression accordingly, allowing these microorganism to behave more like a multicellular organism than a singular cell. Gene expression caused by this mechanism, allows the regulation of several physiological activities which include, virulence, sporulation, symbiosis, biofilm formation, motility, antibiotic production, bioluminescence and conjugation[7]. Bacteria that perform this phenomenon are able to synthesize signaling molecules called autoinducers (AI) and release them to the extracellular matrix. At high cell densities, a certain extracellular concentration of these AIs is attained, allowing detection and response. These AIs are detected by receptors that exist in the membrane or they diffuse through it and are detected in the cytoplasm. The detection of these AIs, besides activating genes for QS dependent functions, also triggers the production of even more AIs, promoting this mechanism in a feed-forward autoinduction[17]. Although the QS mechanism follows this pattern in most bacteria, it differs greatly in the type of AIs and in signal transduction system used by gram-positive and gram-negative bacteria.

Quorum sensing in Gram-Negative Bacteria

2.2.1

In gram-negative bacteria, typically, the LuxI/LuxR-type QS systems are used (homologous to the first described QS system from *Vibrio Fischeri*[18], [19]). In these systems, the LuxI homolog is an AI synthase that catalyzes a reaction with S-adenosylmethionine (SAM) and an acyl carrier protein (ACP) to produce a freely diffusible acyl-homoserine lactone (AHL)-type molecule, which serves as the main signalling molecule. They're constituted by a homoserine lactone ring and a fatty acid side chain, which varies in size (C4-C18), saturation and oxidation at C3 position. As the AHLs accumulate in the extracellular matrix, when the threshold concentration is achieved, the AIs start to diffuse through the membrane and start to bind to the cognate cytoplasmatic transcriptional regulators, LuxT-type proteins, allowing gene expression of a target gene. A QS response is, like this, induced, and besides this, an autoinduce synthethase is positively regulated providing even more AIs.[20]

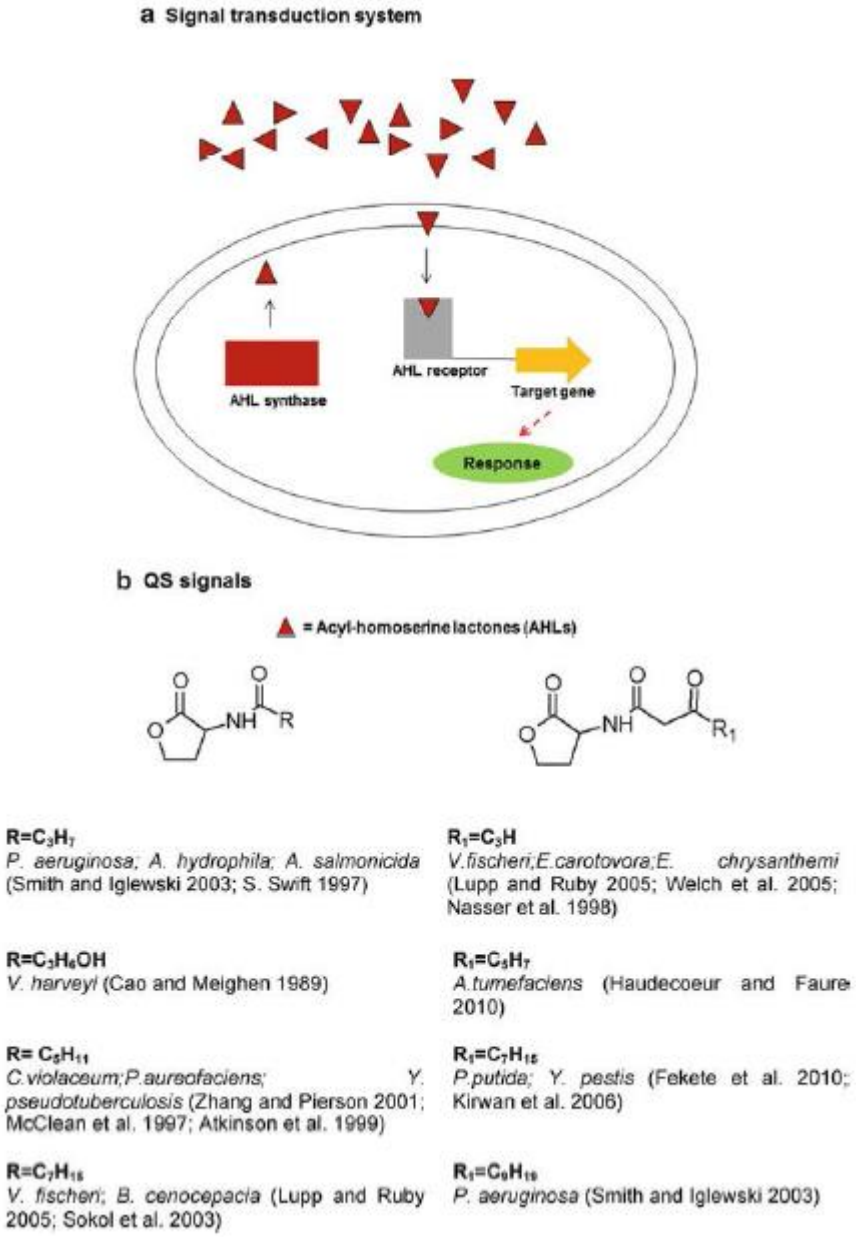

Figure 2.2: Gram-negative bacteria QS signal transduction and AHL structure. (a) QS signal transduction system. AHL synthase and AHL receptor are LuxI and LuxR, respectively. (b) Chemical structure of AHL signalling molecules. Taken from[20]

Quorum sensing in Gram-Positive Bacteria

2.2.2

In gram-positive bacteria, a two-component signal transduction system is the most widely used QS mechanism. The AIs produced are, in this case, autoinducing peptides (AIPs). They're produced as precursors pro-AIP in bacterial cells and excreted through specialized membranes-bound AIP transporters, which process the pro-AIPs to obtain AIPs in the size range of 5-17 amino acids that can be posttranslationally modified, and can be linear or cyclized. The detection is performed via a membrane-associated two-component histidine kinase (HK) receptor. At high concentrations, detection starts to occur. The AIPs bind and activate the HK causing its autophosphorylation, triggering the transfer of the phosphoryl group to a cognate response-regulating protein, which leads to target gene expression[17].

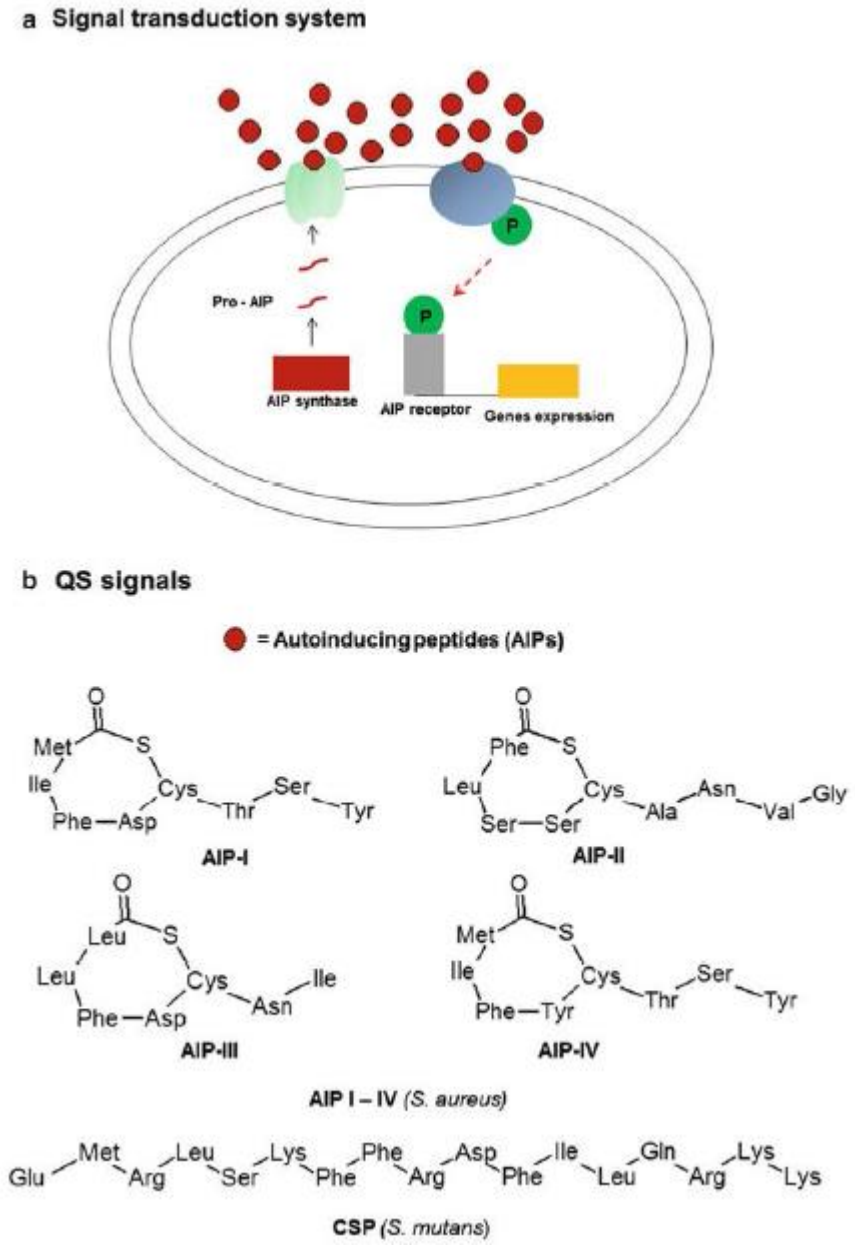

Figure 2.3: Gram-positive bacteria QS system and AIP structures (a) QS system. (b) Chemical structure of AIP signalling molecules. Taken from [20]

2.3 Quorum Quenching – Communication Blockage

Quorum quenching is a type of mechanism that exists in nature which abolishes bacterial infection and other physiological activities of bacteria by interfering with cell-to-cell communication, making it an anti-quorum sensing mechanism.

Some of the QS inhibition strategies are: disruption of efflux pumps, inhibition of QS signal biosynthesis, inhibition of QS signal detection by receptor blockage and **QS signal degradation in the extracellular environment**[20]**.** The last one mentioned is the one relevant for this thesis, so it will be the one explained in most detail.

2.3.1 Disruption of efflux pumps

Bacterial resistance may be developed through efflux pumps (transport proteins), which are capable of expelling to the extracellular environment, certain molecules which would be harmful to them (such as antibiotics).It has been shown that the production of these pumps is QS mediated. This means that an inhibition of the QS mechanisms lead to an effect on the efflux pumps and therefore, it can fight, for instance, bacterial antibiotic resistance[20].

2.3.2 Silencing bacterial communication by targeting the biosynthesis of QS signals

The strategies involved are based on the inhibition of AHL and AIP production in gram-negative and gram-positive bacteria, respectively, for intraspecies communication, as well as inhibition of AI-2 production, that is responsible for interspecies communication. These strategies focus mainly in the inhibition of certain enzymes that are directly involved in the production of the AIs, as without these, the pathway of QS signal production is blocked[20].

2.3.3 Silencing bacterial communication by targeting and blocking the signal receptors

Several QS inhibitors have been developed as analogues of native signals to disrupt the QS pathways by interacting with the receptors of bacteria. These inhibitors compete with the native signals, but, when these molecules interact with the receptors, the signal-receptor becomes inactive, leading to the blockage of the pathway that would lead to gene activation[20]

2.3.4 Quorum Sensing signal degradation in the extracellular environment

2.3.4.1 Antibodies act as scavengers of Autoinducers

Although it is believed that the non-proteinaceous nature and low molecular weight of the AIs should not produce an immune response, a few antibodies have been reported to be able to sequester and neutralize AIs of both gram-positive and gram-negative bacteria. There are still not enough studies to confirm that these molecules have a significant effect on QQ effect.[20]

2.3.4.2 Active Uptake of AI signalling Molecules by Beneficial Bacteria

There have been reports of competitive bacteria, when in the same environment as those who produce AIs for QS, which are able to take in and process these molecules within themselves, therefore acting as a QQ agent[21].

2.3.4.3 Enzymatic Inactivation/Degradation of AIs

This type of inactivation in gram-positive has little reports in the literature to mention, but NADPH oxidase, myeloperoxidase (MPO) and inducible nitric oxide synthase were critical for defense against *S.aureus* capable of quorum sensing, while they weren't effective against a QS deficient mutant[22]. But most of the investigation made on gram-positive bacteria has been focused on targeting the AIP receptors[20].

For gram-negative bacteria though, the signal degradation is one of the most promising methods as it doesn't interfere with survival bacterial mechanisms, providing less selective pressure, and a few enzymes able to degrade/modify AHLs are known. These can be split in two classes. The first one includes an enzyme class that reduces carbonyl groups to hydroxyl, the oxidoreductase. The other class includes the AHL-acylase and the AHL-lactonase, which are capable of breaking the AHL molecule.

OxidoreductaseThis enzyme targets the acyl side chain by oxidating or reducing the AHL, promoting a modification of the molecule as shown in **Figure 2.4** (B), possibly affecting the specificity and recognition of the signal.

AHL-acylase - Already proven in previous studies to have a QQ effect by our laboratory[23] and heterologous expression of AHL acylase genes in P. aeruginosa affected the production of virulence factors and other QS-dependent traits[24]. Its mechanism of AHL degradation irreversibly hydrolyzes the amide linkage between the acyl chain and homoserine moiety of AHL AIs. This separates the lactone ring from the fatty acid chain, as shown in **Figure 2.4** (B), eliminating the QS signal[9]

AHL-lactonase - It is the most relevant enzyme for this thesis and it was the one attempted to produce and purify. The lactonase is capable of hydrolyzing, in a reversible manner, the homoserine lactone ring in the AHL as shown in **Figure 2.4** (B), which makes the molecule incapable of binding to the AI cytoplasmatic transcriptional regulator, reducing considerably the cell-to-cell communication. There are two lactonase families identified in prokaryotes, the AiiA lactonase metallohydrolase and the QsdA lactonase from *Rh. Erythropolis* strain W2[9]. The AiiA was the one selected, as it was produced previously in recombinant *E. Coli*[26], one of the most well characterized microorganisms in the literature, allowing an easier manipulation of the process.

The QQ effect of the lactonase has been previously shown in literature. Expression of an aiiA gene from B. cereus A24 in the opportunistic pathogen P. aeruginosa reduced the content of 3OC12-HSL, prevented accumulation of C4-HSL, decreased the production of extracellular virulence factors, and reduced swarming motility[25].

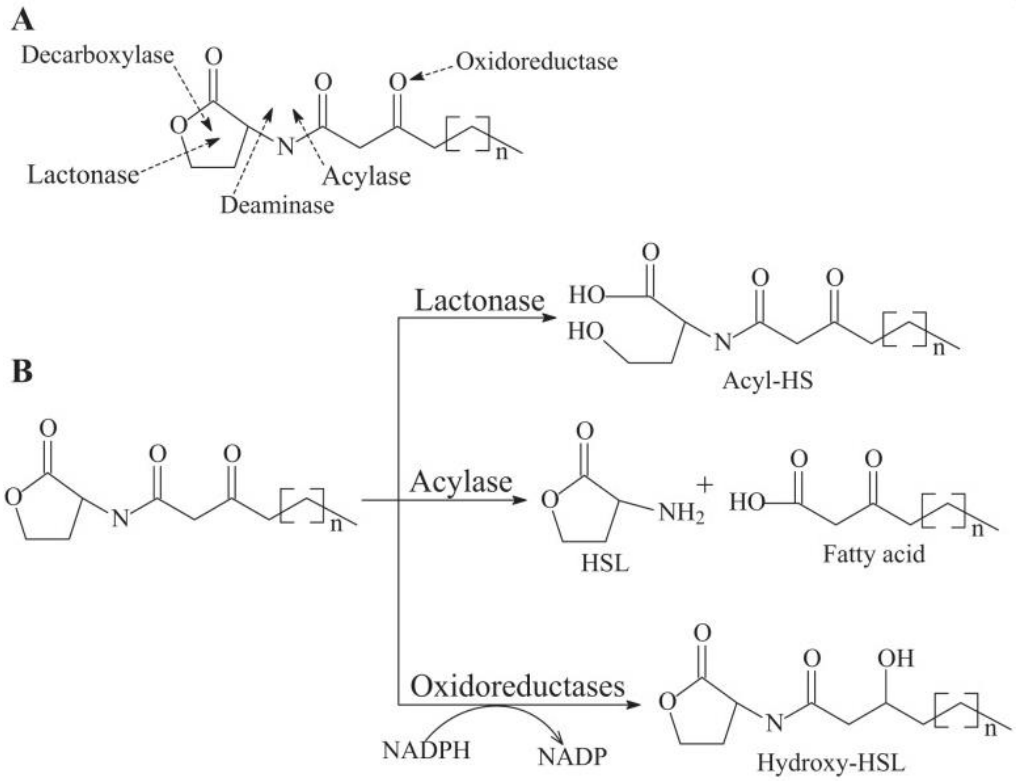

Figure 2.4: AHL cleavage sites and possible mechanisms. (A) - Acyl-Homoserine lactone possible cleavage sites; (B) - Corresponding mechanism of known QQ enzymes. Taken from [9].

2.4 Nanotechnology in Medicine

Most biological molecules, like proteins and DNA function at the nanometer scale. As it works in the same scale, nanotechnology can address several biomedical problems that previous treatments couldn't. This provides us with mechanical, chemical or biological components with improved effectiveness and response, while still being cost effective. Nano components are employed in several fields of medicine like imaging, sensing, drug delivery, gene delivery and artificial implants[27].

One of the major struggles in medicine nowadays, is the emergence of MDR organisms[2][3], which are capable of resisting to several antibiotics, having, that way, an improved virulence. Since antibiotics aren't as effective as they were 50 years ago, new antibacterial treatments have to be developed in order to fight these MDR species, and nanotechnology has the potential to provide exactly that.

2.4.1 Antimicrobial Nanoparticles

Antibiotics have been, and will still be used worldwide, but they fail sometimes when it comes to the troublesome MDR strains and biofilm formation. Antimicrobial Nanoparticles (ANPs) show great promise acting as alternative treatments as ANPs have a lot of modified and inherent chemical properties that allow them to have several types of action mechanisms against microbial, represented in Figure 2.5. Having such a large range of mechanisms, bacteria are unable to develop resistance against ANPs.

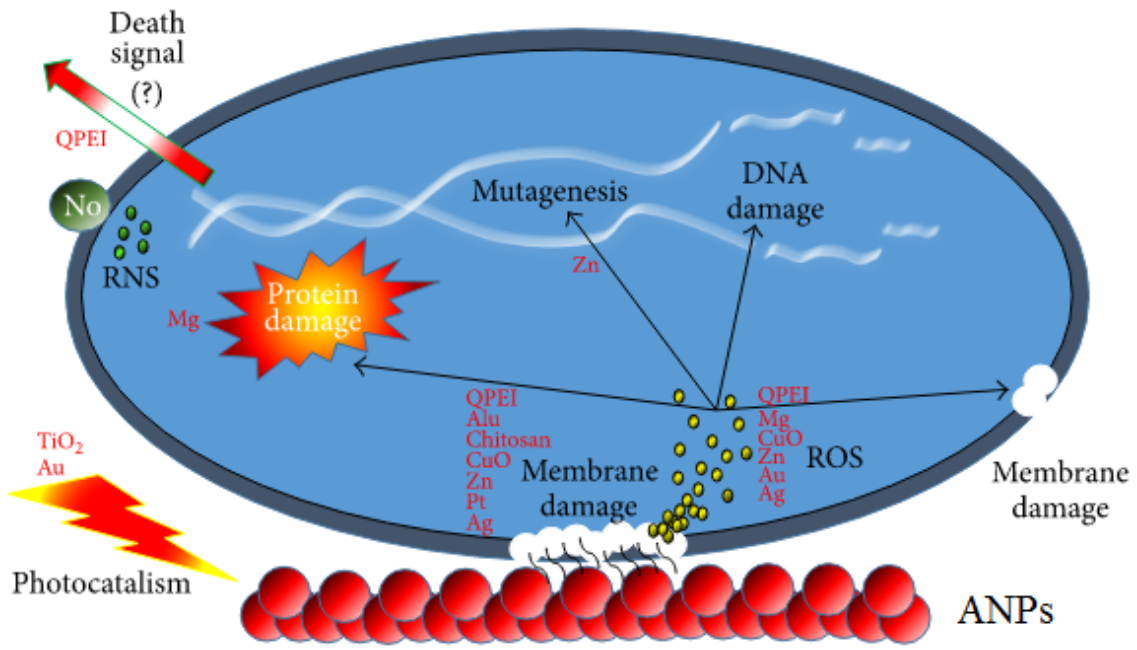

Figure 2.5: Types of mechanism of several types of ANPs; RNS - Radical Nytrogen species; ROS - Radical Oxygen species; QPEI – Polycatyonic ANPs; Addapted from [20]

There are mainly two major lethal pathways, as shown in the **Figure 2.5**. Firstly, when ANPs bind electrostatically to the cell, its membrane potential and integrity is disrupted, leading to a consequent imbalance of transport, impaired respiration, and interruption of energy transduction and/or cell lysis and finally cell death[28]. Secondly, at sufficiently high concentrations, metallic based ANPs release ions, e.g. copper and silver, which induce the formation of reactive oxygen species (ROS), capable of inhibiting DNA replication and amino acid synthesis, leading to cell death[14].

ANPs can be divided in two major classes, based on what type of molecules constitutes them: Inorganic Nanoparticles and Organic Nanoparticles.

2.4.1.1 Inorganic Antibacterial Nanoparticles

Widely studied, metal and metal oxide particles are known to have high levels of antibacterial power. Particles in this class include silver (Ag^+), iron oxide (Fe_3O_4), titanium oxide (TiO_2), copper oxide (CuO) and zinc oxide (ZnO). The main mechanism of cell disruption by these ANPs is the generation of ROS, while some can still be effective due to their physical structure and metal ion release[14]. Bactericidal mechanisms of some of these particles will be explained next.

Silver-containing Nanoparticles (AgNPs)

AgNPs have several antimicrobial mechanisms, being one of the strongest antibacterial metal containing NPs and they're thought to develop a lot less resistance in bacteria then conventional antibiotics. These NPs have antimicrobial activity due to the release of Ag^+ to the solution[28].

The first mechanism is the Ag^+ interaction with sulfur and phosphorus containing groups of proteins of the cell wall and plasma membrane, which creates holes, allowing cytoplasmatic contents to leak, disrupting the H^+ gradient across the membrane. If this still doesn't kill the cells, it still creates openings for the Ag^+ to pass through the membrane, into the cytoplasm, where it has a large range of bactericidal effect, being capable of inhibiting cytochromes of the electron transport chain of microbes, DNA replication and cell wall synthesis in Gram-positive bacteria. They can also damage DNA and RNA, denature 30S ribosomal units and form ROS[28].

Titanium dioxide-containing Nanoparticles (TiO_2 NPs)

At least two antimicrobial mechanisms are known in these ANP. On one hand, TiO_2 cause the formation of ROS upon exposure to near-UV and UVA radiation, in a process called photocatalysis, as shown in **Figure 2.5**. On the other hand , they also show bactericidal activity without the influence of irradiation, although the mechanism behind this phenomenon has yet to be discovered[28]

Iron Oxide and Gold-containing Nanoparticles (Fe_3O_4 NPs and Au NPs)

These are a part of a class of ANPs which generally lack antimicrobial properties but can be modified to introduce these properties. Modified surfaces with Fe_3O_4 NPs showed antiadherent properties, decreasing significantly bacterial colonization. Au NPs, when photothermically functionalized, also

showed antibacterial properties. Au NPs bound to Fe_3O_4 activated photothermically showed higher stability and stronger bactericidal effect[14].

2.4.1.2 Organic Nanoparticles

Organic NPs are composed by polymeric substances which can kill microbial by releasing antibiotics, antimicrobial peptides and enzymes (that have to grafted into the surface), or, be functionalized with highly cationic surfaces which are able to interact with cell wall or membrane, disrupting it. This mechanism depends on several factors, e.g molecular weight, charge density, hydrophobicity, counter ions affinity and pH[13].

Antibacterial Polymers

Polymers like Chitosan, Poly-ε-lysine, 6-deoxy-6-(w-aminoalkyl) amino-cellulose (AC) have a high amount of amino groups, which confer the molecules high polycationic properties, capable of interacting electrostatically with the membranes of bacteria, typically followed by cell lysis[25]–[27].

Polymers attached with Antibiotics

Polyelectrolytes have been reported to be used for the incorporation of antibiotics, having an enhanced effect, as the polymer create openings in the cell membranes, increasing its permeability, allowing the antibiotics to enter the cell and damage it from inside it[13].

2.4.2 Layer-by-Layer films

Layer-by-layer (LbL) self-assembly method first implementation was in 1966 using microparticles [31], forgotten and revitalized later in 1991 with the discovery of its wide range of applicability[32]. The method is based on consecutive alternating depositions of oppositely charged molecules, connecting electrostatically between them, as shown in **Figure 2.6**[33]. With this, ultrathin (nm scale) films are possible to be produced in several materials, increasing its strength and durability, or even confere them special properties, e.g. antibacterial, antiadherent.

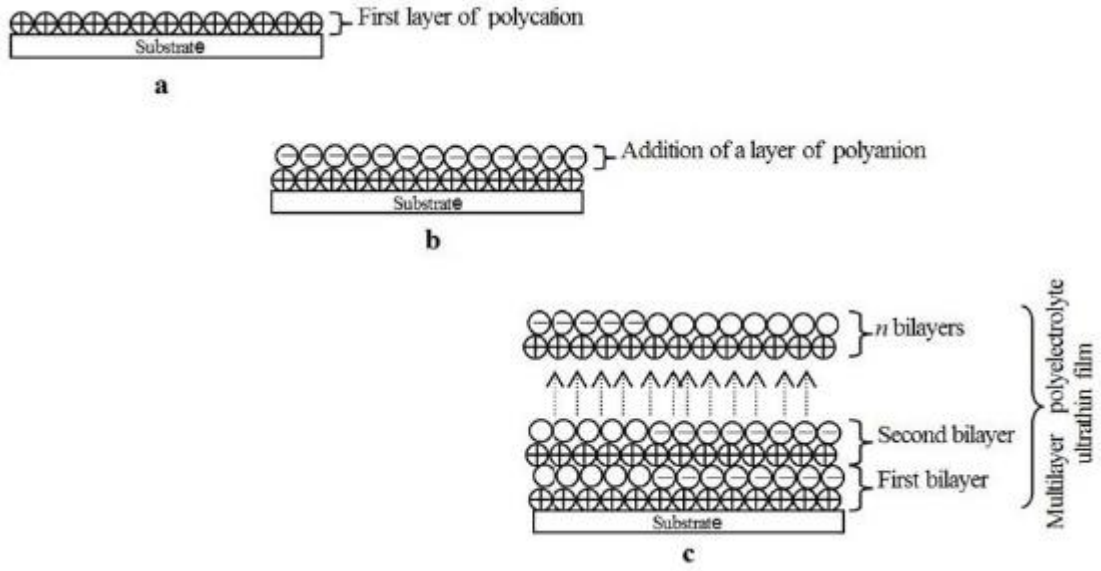

Figure 2.6 - Layer-by-Layer films assembly method. Taken from [33]

2.4.2.1 LbL films as antibacterial coatings

Several types of LbL-based antimicrobial coatings have been reported in recent years. pH controlled-release antibacterial coatings have been produced through the assembly of tannic acid with several cationic antibiotics. These films were capable of releasing these molecules upon pH decrease, inhibiting bacteria adhesion to the surface and their growth[34].

Immobilization and posterior deposition of lysozyme (capable of disrupting the bacterial cell wall or membrane) and gold nanoparticles in cellulose nanofibers was possible through the LbL method, leading to films with excellent antimicrobial properties against both gram-negative and gram-positive bacteria[35].

Quorum quenching and antibiofilm enzymes (acylase and amylase, respectively) have also been immobilized in silicone using LbL with positively charged polyethylenimine alternating with the negatively charged enzymes. These enzymes showed enhanced antibiofilm activity due to the ability of simultaneous action against biofilm components, e.g. QS signals and exopolyssacharide adhesives, resulting in a lower colonization by gram-negative bacteria[11].

2.4.3 LbL Nanoparticles

LbL, recently, has been applied to Nanoparticles, creating multilayers around a single particle, instead of only being applied to films. The method is based on the same principle as the film formation, except that the initial template for the first deposition is a spherical charged core. These cores can be used to graft other molecules to it, or it can be dissolved later, obtaining a hollow core that can be loaded and functionalized (functioning as nanocasules). This can also be said about the polyelectrolytes, which can have other molecules attached to each layer, according to the final objective[36].

2.4.3.1 LbL Nanoparticles as antibacterial particles

Despite LbL Nanocapsules little amount of reports as a novel antibacterial system, some studies have started to appear and showed great potential.

A biohybrid nanoparticle system that included antibiotic, enzyme, polymer, hyaluronic acid and mesoporous silica nanoparticles showed an effective bactericidal response *in vitro* and *in vivo* against both gram-positive and gram-negative bacteria, and also good biocompatibility and low hemolytic side effect[37].

Helicobacter pylori are one of the major causes of gastric cancer. A system with advantages of both vesicular and particulate carriers was prepared through alternating layer depositions of poly (acrylic acid) as the polyanion, and poly (allylamine hydrochloride) as the polycation and liposomes as the core gave a prolonged release of amoxicillin and metronidazole, having produced high antibacterial activity. This system proved to have commendable potencial when compared to other *H. pylori* eradication treatments[38].

2.5 Layer-by-Layer Nanoparticles and Quorum Quenching enzymes

Nanoparticles have been shown to be revolutionary in several fields. The biomedical area is no exception, because NPs, by themselves, can be directed to specific targets (like bacteria), inducing specific responses. For the specific topic of this thesis, the wished response was an antibacterial activity by the NPs. Organic polymer and metal-containing NPs have been shown to have this property enhanced when compared to conventional delivery methods of different bactericidal molecules.

Layer-by-Layer brings the enhancement of this effect to another level, capable of joining the effects of antibacterial NPs and polymers in the same surface and in several layers, improving not only the antibacterial capacity, but also have a more prolonged time of action.

LbL systems exist in two forms: films and NPs. The first one has been better characterized and has been used in several applications, but can only be used in solid surfaces. While the second one still has room for improvement of the production technique but its potential is bigger as it can be applied in solutions, creams or lotions.

Besides polymers and NPs, LbL can incorporate several other molecules, e.g. antibiotics, enzymes, signaling molecules and others. In the enzymes capable of antibacterial activity category we have enzymes that degrade cell walls, matrix-degrading (MD) enzymes, and quorum quenching (QQ) enzymes. And MD and QQ enzymes have been already used in hybrid LbL systems and proven to work together enhancing antimicrobial activity[11].

This thesis purpose was to be a starting point in creating a hybrid LbL system with Nanoparticles, using a biocompatible polymer with antibacterial activity (6-deoxy-6-(w-aminoalkyl) amino-cellulose (AC)), merged with quorum quenching enzymes (and possibly other enzymes and molecules) with the purpose of its application in creams and lotions for skin care applications.

For that, a production and purification protocol was performed and optimized for lactonase, a QQ enzyme which degrades AHLs produced by gram-negative bacteria. Also, a protocol was developed for Layer-by-Layer NPs assembly, with the polycation being the AC, which has antibacterial properties due to its high amount of amino groups that confer a high positive charge to the polymer, and serving as structural support and polyanion, Hyaluronic Acid was chosen. The core was made out of commercial Gantrez polymer Nanoparticles.

3 Materials and Methods

3.1 Materials

Gantrez Nanoparticles Layer-by-layer

All reagents and media were provided by Sigma-Aldrich unless specifically stated.

3.1.1 The Gantrez Nanoparticles (NPs) were kindly provided by Bionanoplus. Cationic derivative of cellulose, 6-deoxy-6-(ω-aminoethyl) aminocellulose (AC, ~15 kDa), was synthesized from microcrystalline cellulose (Fluka, Avicel PH-101) via a tosyl cellulose intermediate, using a previously described procedure [30], [39]. Prior LbL assembling, aminocellulose solution (20g/l) was diluted to 5g/l in mQ water and then filtered through a 0.45 μm syringe filter in order to remove any impurities. . Negatively charged hyaluronic acid (HA) with average Mw~75.7 kDa and 8.29 kDa were obtained from Lifecore Biomedical (USA) in the form of its sodium salt. Dimethyl sulfoxide, Fluoroscein isothiocyanate, Na_2CO_3, $NaHCO_3$, NaOH and HCl were used without purification.

Antibacterial Activity

3.1.2 Gantrez Nanoparticles Layer-by-Layer previously prepared in the laboratory, Mueller Hinton (MH) broth, Centrimide Agar broth, Braid Parker broth, *Streptomyces aureus* plate culture. *Pseudomonas Aeruginosa* plate culture and KH_2PO_4 buffer solution.

3.1.3 Lactonase Cloning, Expression and Purification

For bacterial maintenance and growing: Luria Bertani (LB) media, LB agar and Super Optimal Broth, were used according to the supplier directives. Auto-inducing media was prepared by mixing phosphate buffer 0.1M, 2%(w/v) Tryptone, 0.5% (w/v) yeast extract, 0.5%(w/v) NaCl containing filtered sterilized 0.05% (w/v) Glucose, 0.6% (v/v) Glycerol and 0.02% (w/v) Lactose.

Buffers used for bacterial resuspension and protein purification and characterization: Bacteria were resuspended in Resuspension Buffer 50mM (HNa_2PO_4/H_2NaPO_4) at pH7.9 containing 500 mM NaCl, 10 mM Imidazole and 100 μM PMSF (Phenylmethylsulfonyl fluoride). Protein purification was performed in the same buffer but at different imidazole concentrations (10 (Binding Buffer), 50, 100, 150, 200, 250, 300, and 500 mM). For SDS-electrophoresis gel the buffers were: Resolving gel (0.1% Ammonium persulfate (APS), 0.5% N,N,N',N'-tetramethylethane-1,2-diamine (TEMED), 0.75M Tris-HCl (1.5M pH 8.8), 0.1% SDS and 12 % Acrylamide/Bisacrylamide (Bio-Rad)), Stacking gel (0.1% APS, 0.5% TEMED, 0.125M Tris-HCl (0.5M pH 6.8), 0.1% SDS and 5% Acrylamide/Bisacrylamide (Bio-Rad)), 4x protein loading buffer (0.0625 M Tris, 2% SDS, 10% Glycerol, 0.4 M DTT (1,4-Dithiothreitol), 0.1% Blue Bromophenol dissolved in destilled water (ddH2O)), running buffer (3 g Tris, 14.4 g Glycine, 1 g SDS, rise with ddH2O up to 1 L and adjust to pH 8.3). For protein detection: Coomassie brilliant blue solution (10% (v/v) Methanol, 10% (v/v) Acetic acid and 0.025% (w/v) Coommasie blue G), Coomassie destaining solution (400 ml Methanol, 100 ml Glacial Acetic Acid and rise with ddH2O up to 1 L). Western-blot was carried out by utilizing the following buffers: Transfer buffer (25 mM Tris, 192 mM glycine, 10% methanol). TBS buffer (8.7 g NaCl, 1.21 g Tris, 0.4 ml HCl in 1L ddH2O, pH 8.0) and TTBS buffer (1 ml Tween 20 dissolved in 1L TBS solution). Reagents used for

western-blot are; Horseradish peroxidase (HRP) conjugated to anti-mouse secondary antibody, anti-HISTag Mouse IgG antibody and super signal west pico chemiluminescent substrate (Thermo Scientific).

For DNA detection: Tris-acetate-EDTA (TAE) buffer (10x): 48.4 g Tris Base, 7.44 g EDTA dissolved in 800 ml ddH2O, 11.42 ml Acetic acid was added and rise with ddH2O up to 1 L. Ethidium Bromide (EB) buffer: 2 µl EB dissolved in 100 ml 1x TAE buffer.

3.2 Methods

Layer-by-Layer Nanoparticles Assembly Concept

Fabrication of this type of particles, is based on the consecutive deposition of oppositely charged polymer layers around a spherical template (also charged) functioning as the core of each particle, which allows the first layer to attach. In the end, depending on the purpose, the core can be dissolved, obtaining particles with a hollow cavity, which can be loaded with components of interest[36].

3.2.1

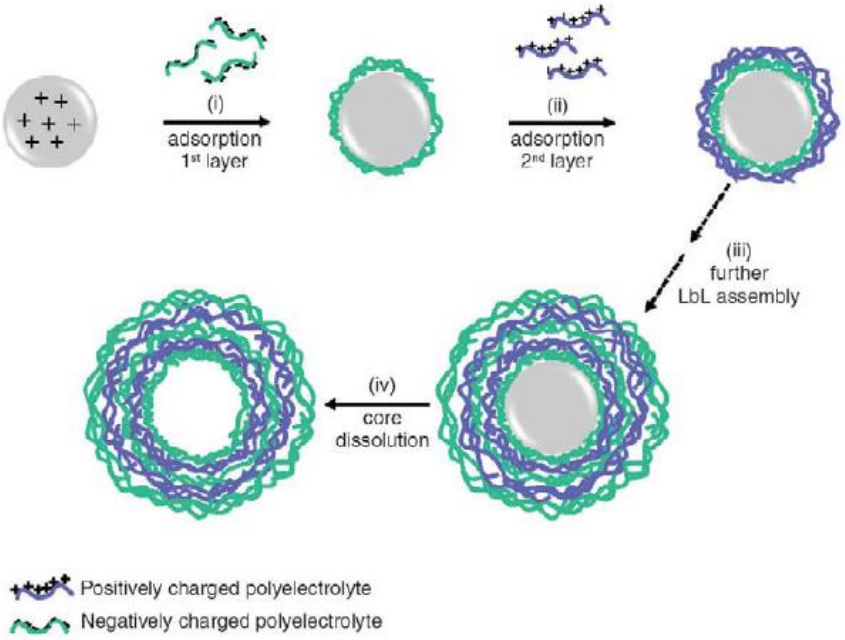

Figure 3.1 - LbL Nanoparticles Assembly process through consecutive oppositely charged polyelectrolyte deposition. Note that the process can also be performed for cores that have negative charge, being the first polyelectrolyte deposited positive, and the second one negative. Addapted from [36]

In order to understand if a good assembly is occurring, usually, several measurements are made to follow the layer growth of polyelectrolytes onto the spherical templates. These measurements are made usually by techniques based on electrophoretic mobility and light scattering. Specifically, Zeta Potential, Mean Size and Polydispersity Index are measured for the template and after every polyelectrolyte deposition.

Bridge Flocculation - In order to obtain stable and well defined nanoparticles, it is needed to avoid bridge flocculation, which is the process where a polyelectrolyte chain connects to more than one nanoparticle, and, consequently, several particles aggregate (Figure 3.2).

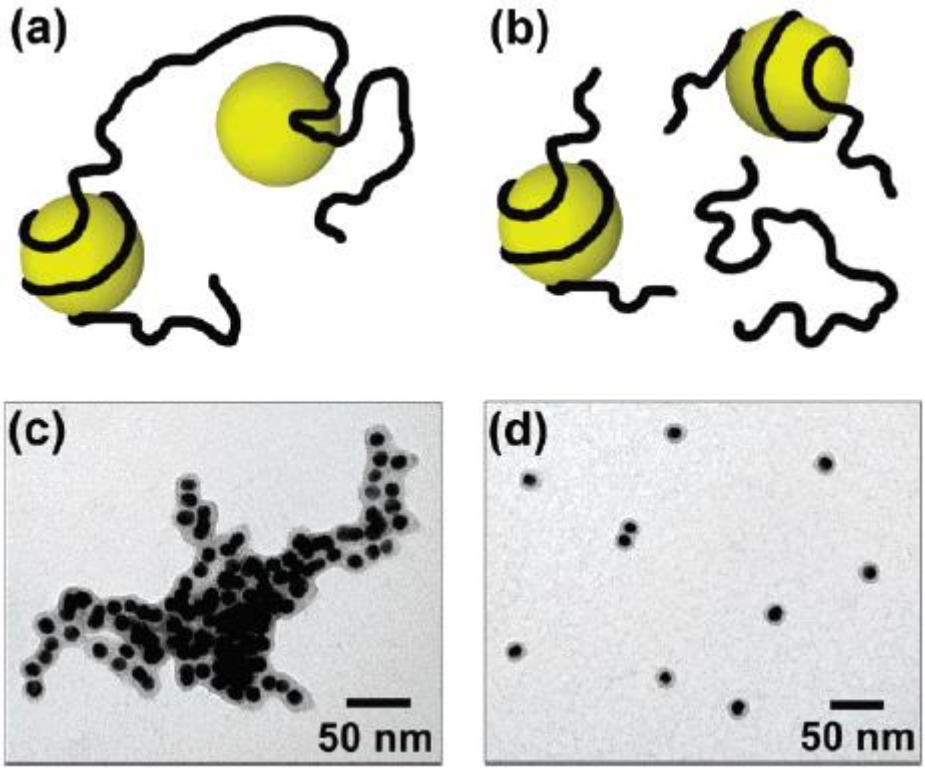

Figure 3.2 – Representation of Bridging Flocculation; Oversimplified Representations of Particles Being Aggregated by Bridging Flocculation (a) and Being Individually Wrapped by Polymer Chains (b); Lower Part Shows Electron Micrographs of Aggregated Particles (c) and of Particles Predominantly Ensheathed Individually (d). Addapted from [40]

There are three important parameters that are expected to play a major role in this, and those are: the length of the polyelectrolyte (which is a function of the degree of polymerization), the average distance between particles (which is adjusted via nanoparticles concentration) and finally, the stoichiometric excess of either nanoparticles or polyelectrolyte chains[40].

Depending on the charge stoichiometry between particles and polyelectrolytes, it is possible to identify three distinct regimes.

Regime I) Colloids >> Polyelectrolytes; Results in incomplete nanoparticle surface coverage and very few polyelectrolyte chains remain in suspension. This would be ideal, as the NPs are covered by the polymer, while little excess of it remains, allowing the deposition of the next layer. But, in this regime, the suspension is usually weakly stabilized and because the colloidal surface has little coverage, it also has little functionality, which doesn't favor the next layer adsorption.

Regime II) Colloids ≈ Polyelectrolytes; Known as the flocculation regime, it has to be avoided as it is close to stoichiometric conditions.

Regime III) Colloids << Polyelectrolytes; Excellent surface coverage and high suspension stability; not requiring high dilutions during the adsorption. The problem here is the high amount of free polyelectrolyte that remains in suspension after the layer adsorption.

Although the most desired regime is the I, it would be very difficult to produce multilayered particles. That way, the most practical approach is to work on regime III conditions.

In general, in this regime, the adsorption of the layer would be favored to the bridging flocculation if the NPs are sufficiently separated from each other (particle concentration influence)[40].

3.2.1.1 **Zeta Potencial** (ζ-Potencial)

When a particle has a net charge on its surface, the concentration of counter ions (ions of opposite charge of the particle) start to increase around the particle. Due to those interactions, a double electrical layer is formed around each particle. This layer is comprised of an inner region (the Stern Layer), where the ions are strongly attached to the particle surface, and an outer region, where they are less attached. The boundary that separates these two regions is called the surface of hydrodynamic shear or slipping plane, and the potential existing in this boundary is called Zeta Potential (ZP). [41]

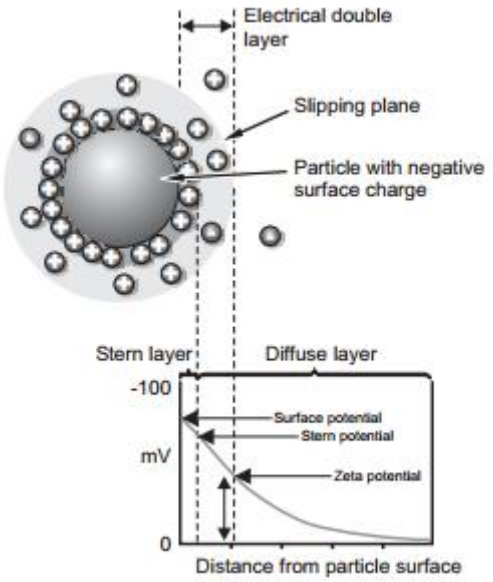

Figure 3.3 - Representation of the electrical double layer formed around charged particles and respective potentials. Taken from [40].

As it is shown in the **Figure 3.3**, the ζ-Potential does not correspond to the real surface charge, but corresponds to the charge after the blinding effect inside the slipping plane is considered.

In order to know what the ZP of a particle is, an electric field is applied across an electrolyte and the charged particles are attracted to the electrode with the opposite charge. The media viscosity tends to oppose this movement. When both these forces enter equilibrium, particles move with a constant velocity, which is named **electrophoretic mobility**.

This mobility is dependent on the dielectric constant of the media, strength of the electric field, the previously mentioned viscosity and finally, the Zeta potential. This way, it is possible to calculate ZP through application of the Henry equation[41]:

$$U_E = \frac{2.\varepsilon.\zeta.f(ka)}{3\eta}$$ **(**Equation 1 - Henry's Equation)

- ζ : Zeta potential
- U_E : Electrophoretic mobility
- ε : Dielectric constant
- η : Viscosity
- *f(ka)* : Henry's function. Which is 1.5 when ZP is measured in aqueous media and moderate electrolyte concentration (Smoluchowski approximation) and it is 1.0 for small particles in low dielectric constant media (Huckel approximation), generally applied in non-aqueous media.

In this work, mQ water was the media used every time the ZP was measured, so, the values of ε, η and *f(ka)*, at 25ºC were 78.304[42], 0.89x10^{-3} kg/(m.s)[43] and 1.5, respectively.

3.2.1.2 Size measurement: Dynamic Light Scattering (DLS)

Also referred as Photon Correlation Spectroscopy or Quasi-Elastic Light Scattering, DLS is a technique for measuring the size of particles below the micron range.

DLS measures the Brownian motion and relates it to particle size. The Brownian motion is the random movement of particles, either in liquid or gas, caused by irregular thermal movements of other molecules colliding with these particles[44]. The larger the particle, the slower the Brownian motion, as the small molecules that surround the big particles, don't have enough kinetic energy to make the big particles move significantly. The reverse happens with the smaller particles, where the solvent molecules have more influence. This way, as viscosity of the media influences the movement as a resistance force, a highly controlled temperature is needed, as the viscosity is related to the temperature. A stable temperature throughout the sample is also very important, so that the convection currents don't cause non-random movements, possibly providing a false interpretation of particle size.[45]

DLS diameter is a value that refers to how a particle diffuses within a fluid, the hydrodynamic diameter, and it is calculated through the Stokes-Einstein equation:

$$d(H) = \frac{k.T}{3\pi.\eta.D} \qquad \text{(Equation 2 – Stokes-Einstein Equation)}$$

- *d(H)* : hydrodynamic diameter
- *D* : translational diffusion coefficient (Brownian motion velocity)
- *k* : Boltzmann's constant
- *T* : absolute temperature
- η : viscosity

DLS observes the time dependent fluctuations in scattering intensity caused by constructive and destructive interference resulting from the relative Brownian movements of the particles in the sample, allowing the average particle size to be calculated.

3.2.1.3 Size measurement: Nanoparticle Tracking Analysis (NTA)

NTA is a technique that is also based on the DLS principles, but it measures the particle movement through image analysis, tracking the movement on a particle-by-particle basis (**Figure 3.4**), which can be related to particle size. It is capable of measuring not only size, but also particle count and concentration, as the sample is measured in a known volume [46].

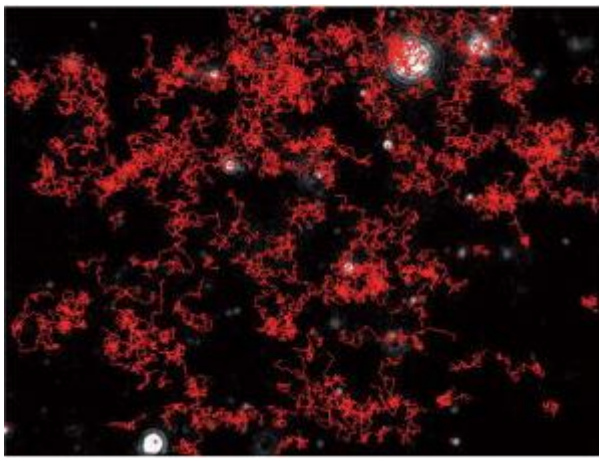

Figure 3.4 - Typical image of NTA analysis. Red random oriented lines represent the Brownian motion of each particle in a set period of time. Taken from [46]

3.2.1.4 NTA vs DLS

Table 3-1 - NTA and DLS differences. Adapted from [47]

Characterization	Nanoparticle Tracking Analysis (NTA)	Dynamic Light Scattering (DLS)
Size Range (nm)	10-1000	2-3000
Size Resolution	1:1.33	1:3
Size Distribution	Works in a known volume, allowing size distribution to be a number distribution and relative particle concentration can be determined	Intensity distribution can be converted to volume distribution but no particle concentration can be accurately calculated
Refractive Index	Requires no information on this parameter	Require information on this parameter. Bias towards more refractile particles

The two methods, despite being based in the same principles, they have several differences as seen on Table 3-1. When the samples are monodisperse (all, or most particles, have the same size) or polydisperse (several populations of different sized particles exist), the most reliable method has to be chosen in order to obtain more reliable data.

Monodisperse Sample

In this case, for DLS, there is no intensity bias. The average size is produced from a large number of identical particles, providing an accurate and reproducible measurement. In contrast, NTA distribution is based on a small number of particles when compared to DLS, potentially generating a less statistically robust result[47].

Polydisperse Sample

On one hand, in DLS, all particles are measured at the same time, and it generates an average size biased towards larger particles as these scatter light more intensely than the smaller particles. On the other hand, NTA, being a particle-by-particle type of analysis, there is no bias of the average towards bigger particles and it allows the discretion of different sized populations of particles[47].

Preparation of LbL AC/HA Gantrez Nanoparticles using Centrifugal filter units (30kDa)

In order to study the LbL buildup on the NPs using fluorescent microscopy, the positively charged AC was labeled with Fluorescein isothiocyanate(FITC). For this, AC should be prepared as a solution of at

3.2.2 least 2mg/ml in 0.1M sodium carbonate buffer. The FITC dissolved in anhydrous DMSO (1mg/ml) was then added to the AC solution (50µl of FITC/DMSO solution per ml of AC solution), and at a rate of 5µl (one drop) at a time while gently stirring. The solution was incubated for 8 hours at 4 ºC, and the unbound FITC was removed using PD-10 desalting column (GE Health Care Sciences), obtaining a final concentration of 3.5 g/l. The pH of the Gantrez NPs, HA and AC solutions was adjusted to 4.5 with 1M NaOH and 1M HCl. For the 1st layer the AC-FITC was diluted to a concentration of 1.8g/l. The first polyelectrolyte was deposited as follows: 100µl of 10x diluted Gantrez NPs 1.98x10^{14}NP/ml were mixed with 1900 µl FITC-AC (1,8 mg/ml) and then, in a 2ml Eppendorf, the reaction was allowed to occur for 20 min in the dark with no agitation. The sample was then transferred to an Ultra Centrifugal filter unit of 30kDa and centrifuged at 4000g for 10 min. The flow-through fluorescence was measured at a gain of 100, and the retentate was resuspended in 2 ml mQ water (pH 4.5) and centrifuged again to remove the non-deposited FITC-AC (first washing step). The washing steps were repeated until the flow-through fluorescence decreased significantly compared to the first washing step. Then the resulting NPs with an AC layer were characterized using fluorescent microscopy and Dynamic Light Scattering (DLS)). For the deposition of the 2nd layer on the AC coated NPs HA, (Mw ≈8.29 kDa) three different concentrations were used: 0.5, 1.0 and 1.5 mg/ml. After 20 mins the procedure of washing the free HA was repeated as described for the AC layer deposition, but the centrifugation was performed for 20 mins. The alternating AC with HA was repeated until the desired number of layers was obtained.

3.2.3

Preparation of the LbL Gantrez AC/HA Nanoparticles using ultracentrifugation for washing

Several dilutions of Gantrez NPs were prepared (1.98x10^{12}NP/ml, 9.9x10^{11}NP/ml and 4.95x10^{11} NP/ml, corresponding diluting the sample 2000x, 4000x and 8000x, respectively). For the 1st layer, 4 ml NPs, were mixed with 4 ml AC (3.5g/l) in 15 ml falcons. The samples were then agitated at 85 rpm for 5 mins and left for 45 mins without agitation for polyelectrolyte deposition. Afterwards, the samples were purified using ultracentrifuge at 18 000 rpm for 20 mins. The pellets were resuspended in 4 ml mQ water (pH 4.5) and transferred to a new falcon. The 2nd layer was formed with 4 mL 3.5 g/l HA (75.7kDa) solution and centrifugation only for 15 mins. The changes in the surface charge and the size

3.2.4 were monitored after each deposition step with DLS and Zeta Potencial. This procedure was repeated until the desired number of layers was obtained.

Antibacterial Activity

Turbidity-based microdilution assay in MH broth: 75 µL Mueller Hinton (MH) broth were added to column 2-12 of a sterile 96 well-plate.150 µL of LbL NPs (triplicate for all LbL NPs) were put in column 1 before transferring 75 µL of the LbL NPs (column 1) to column 2 and mixed. After mixing, 75 µL of the samples from column 2 to column 3, mixed again and the process was repeated down the length

of the plate until reaching column 12. Bacteria (*Streptomyces aureus* and *Pseudomonas aeruginosa*), previously grown overnight in MH, was diluted to OD (600nm) =0.01 in MH and 75 µL of bacterial inoculum was added to each well. Absorbance was measured at 600 nm (0 time) and incubated plate overnight at 37 °C and 230rpm. Controls were also made in triplicates: Negative control = 75 ul MH + 75 µL bacteria (OD=0.01); Positive control = 75 µL (gentamicin 100 µg/mL) + 75 µL bacteria (OD=0.01); Sterility control = 150 µL MH; Gantrez Control: 75 µL Gantrez + 75 µL MH.

On the next day, the absorbance of the samples was measured again at 600nm, the difference between time 0 and the next day was calculated and the turbidity of the samples was compared with the controls.

Spot Plating: 30 µL from *P. aeruginosa* and *S. aureus* inocula were serially diluted using 180 µL of 0.3mM KH_2PO_4 sterile buffer solution. The cultures were spot platted (the one that were serially diluted) on agar plates – Cetrimide for *P. aeruginosa* and Braid Parker *for S.aureus*. Incubate for 24 h at 37 °C.

After 24h, CFU were counted in order to ascertain the how much of growth inhibition.

3.2.5 Lactonase Cloning, Expression and Purification

Amplification of the Lactonase containing vector: Larger amounts of lactonase gene were obtained by transforming the vector into *E. Coli* DH5α competent cells through a heat shock at 42ºC for 1 min and plated overnight in LB agar + Ampicillin (100µg/ml) at 37ºC. Upon growing of a colony in LB broth + Ampicillin, the vector purification was performed according the **QIAprep Spin MiniPrep** protocol (described in appendix 7.1).

DNA characterization: Two different techniques were used in order to analyze DNA purity and stability; UV-visible spectroscopy and agarose gel electrophoresis: Spectroscopic characterization of DNA was carried out in a Cary 100Bio spectrophotometer (Varian, Australia). All spectra were recorded in the 200 nm – 350 nm range with a bandwidth of 2 mm, a response time of 0.1 s, and a scan speed of 300 nm/min. Electrophoretic analysis was performed by preparing a 1% (w/v) agarose gel in 1X TAE buffer and microwaved until agarose was completely melted. The agarose solution was cooled down nearly to 55ºC - 65ºC, which normally took 10 min, and poured down into a gel tray containing a comb to form the wells. After complete gel solidification, the DNA samples were loaded together with 6x DNA loading buffer, and run in TAE buffer at 70 V for 80 min by an electrophoresis system (Bio-Rad). The gel was incubated in EB buffer, which intercalates between the nitrogenous bases, for 30 min and an image system (Bio-Rad) was used to visualize the DNA fragments upon UV irradiation.

Lactonase Expression: Gene aiiA coding for lactonase from *Bacillus sp. isolates A23* [Reimann et .al, 2002] was cloned into a pET22b plasmid for expression in *E.coli* by a commercial service (GenScript, USA) through *MscI* and *XhoI* restriction sites. This vector contains a 6xHisTag fused downstream the gene for purification by immobilized metal affinity chromatography. Chemically competent *E. Coli* BL21 (DE3) cells were transformed through heat shock and plated overnight in LB agar + Ampicillin (100µg/ml) media at 37ºC. Several colonies were picked and each incubated in different falcons with LB + Ampicilin (100µg/ml) overnight (between 16 and 18h), at 37ºC and 230 rpm. One falcon was

chosen, while the remaining were stored at -80ºC for further analysis, and diluted to 0.05 Absorbance (at λ=600nm) in 50ml LB, split in five 50 ml falcon (10 ml culture each) to facilitate aeration and incubated at 37ºC and 230rpm until they reached an absorbance of ≈0.7. Different Isopropyl β-D-1-thiogalactopyranoside (IPTG) concentrations (between 0.1mM to 1.0mM) were then added to the different cultures and incubated overnight at room temperature and 230 rpm. The samples were centrifuged at 4000 rpm for 20 min, the supernatant was discarded and the pellet was resuspended in resuspension buffer, and sonicated 5 times for 30 s at a 30% amplitude in a sonicator of 750W. The lysed cells were centrifuged at 35000rpm for 35 min and the soluble part (supernatant) was loaded to a SDS gel (optionally, the pellet can also be loaded into the gel to analyse the insoluble part) and ran at 100V for ≈2 hours. For Coomassie assessment, the gel was stained overnight with Coomassie Blue and destained with Coomassie destaining solution the next day. In Western Blot analysis, the transference occurred for 30 min at 15V, to a nitrocellulose membrane (0.45 µm porus size, from Bio-rad). For detection, an anti-HisTag Mouse IgG antibody was applied, followed by a HRP conjugated anti-mouse antibody. Development was performed using super signal west pico chemiluminescent substrate according to the manufacturer. Both detailed protocols for either Coomassie staining and Western blot are in appendix 7.3 and 7.2.

Autoinducing protocol: The same protocol as the IPTG one was followed, with the difference that instead of using 50ml media (split in 5 falcons, 10ml each), the falcon culture would be mixed in 200ml of autoinducing media and grown overnight at 37ºC and 230rpm.

Lactonase Purification: Purification was performed in a Column HisTrap™ HP (1 ml) from GE. Prior to sample loading, several column volumes of binding buffer were used for column equilibration. Then, sample was loaded and the flow-through (FT) collected for further analysis. For washing, around 3 ml of 300mM imidazole buffer were loaded and FT collected. Finally, protein was eluted by utilizing 3ml 500mM imidazole buffer. For final wash and column storage, binding buffer containing 20% (v/v) ethanol was used.

For gradient purification, the same protocol was followed, with the difference that several washing steps were performed employing 50, 100, 150, 200, 250, 300mM imidazole concentrations to determine the imidazole concentration where the protein would be eluted.

4 Results and Discussion

4.1 Gantrez nanoparticles as a template for LbL assembly

Table 4-1 - Gantrez Particles Characterization. Mean Size was measured using NTA and DLS, concentration was measured through NTA and PDI was measured through DLS, while Laser Doppler Micro-Electrophoresis was used to measure the Zeta Potencial.

NP concentration (NPs/ml)	$3.96x10^{15}$±$6.48x10^{14}$
Mean Size-NTA (nm)	134.8±31.3
Mean Size-DLS (nm)	96.63±14.20
PDI	0.0864±0.0122
ZP (mV)	-19.10±0.52

Prior AC/HA multilayers deposition on commercially available Gantrez nanoparticles (NPs) their concentration, size, PDI and surface charge were analyzed. The DLS data show that the polyelectrolytes assembly was made starting with a stable monodisperse suspension (PDI lower than 0.1) containing small size particles of about 100 nm, while the NTA shows a value around 30nm larger. But, in this case, as we have a monodisperse sample, the most reliable method is the DLS[47]. In addition the zeta potential at pH 4.5 revealed the negatively charged NPs – a key characteristic, consequently defining the first polyelectrolyte layer deposition. The Zeta Potencial also shows a high negative charge, which confirms the fact that the AC polyelectrolyte easily attaches and envelops the NPs for the 1st layer deposition. Therefore, these particles might be used as a template for the formation of antibacterial HA/AC multilayers formation.

4.2 Characterization of LbL AC/HA Gantrez Nanoparticles

Particles obtained by two methods were characterized. Firstly, NPs were washed after each PE deposition with ultracentrifugal units with 30KDa pore size. And secondly, ultracentrifugation was used in order to purify the particles after each PE adsorption.

4.3 NPs washing with Ultra Centrifugal filter units (30kDa)

In this experiment, there were a few problems related with aggregates formation, which caused the filter to get NP's stuck to it, consequently NPs were lost and the filters, after a certain amount of layers (3 or 4) got stuck and the experiment had to be stopped. That's why the maximum was only up to 4 layers.

4.3.1 Fluorescence Microscopy

Control – Aminocelulose + Hyaluronic Acid

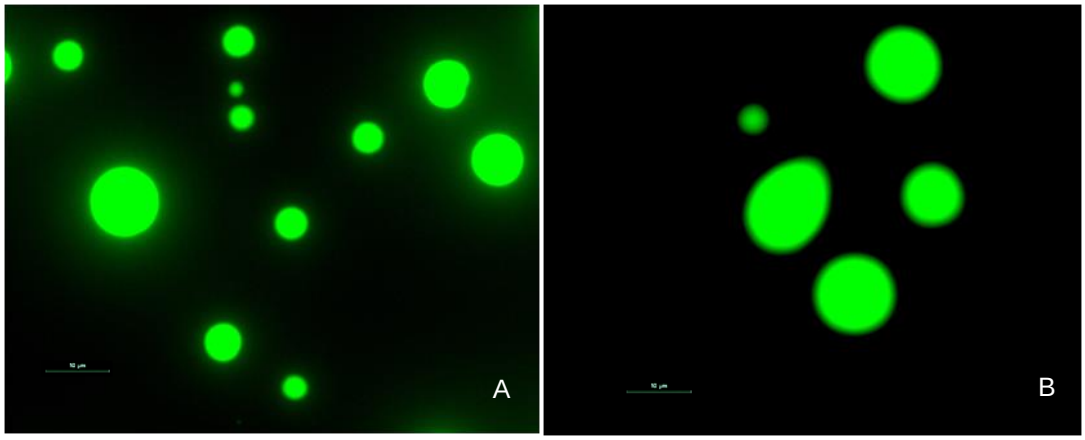

Figure 4.1 - Visualization of the AC/HA complexes through Fluorescence Microscopy. Scale is 10µm wide. (A) 75µl AC(5g/l) + 75µl HA (2g/l); (B) 150 µl AC (5g/l) + 75 µl HA (2g/l)

This control experiment had the purpose of checking what happened when the oppositely charged polymers were mixed. Fluorescence microscopy images revealed the formation of complexes between HA and AC - big aggregates with diameters in the order of the µm. There is also a notable difference in both images, as in the right image, a bigger size of complexes are formed when compared to the left one. That is explained with the larger amount of AC in solution, which allows a larger amount of it to complexate with the HA.

NP's layering for samples with different Hyaluronic Acid Concentrations

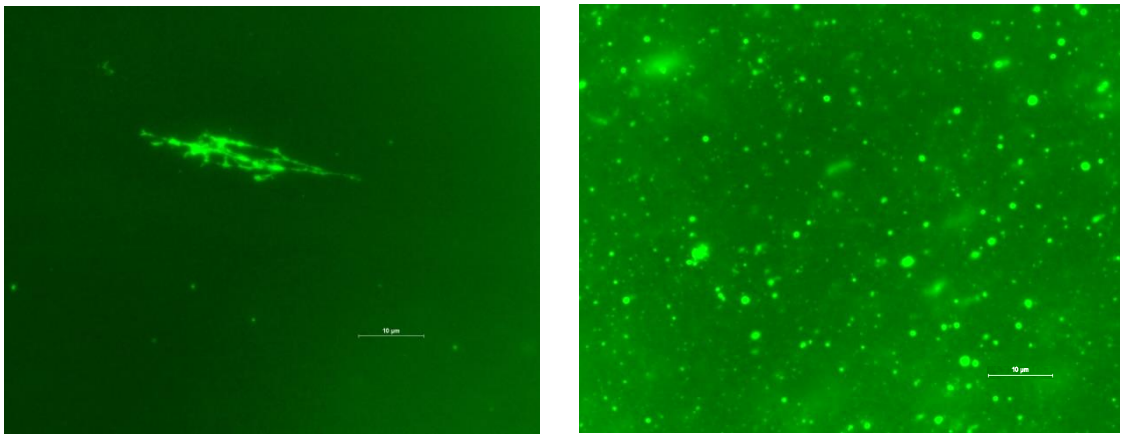

Figure 4.2 - LbL AC/HA Gantrez NPs with 4 layers, HA (0.5mg/ml) on the left, and with 4 layers, HA (1.0 mg/ml) on the right Scale is 10µm wide.

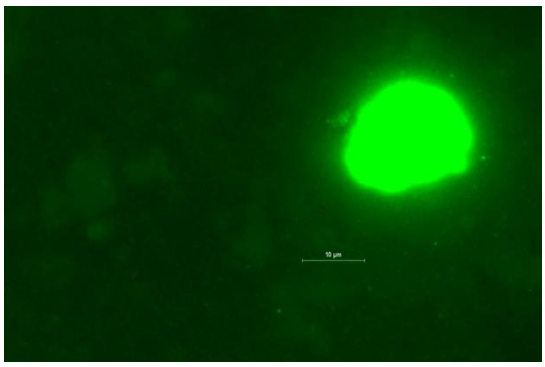

Figure 4.3 - LbL AC/HA Gantrez NPs with 3 layers, HA (1.5mg/ml). Scale is 10µm wide.

As it is can be seen from the fluorescence microscopy images, the method for coating otherwise inert (no functional group present) surface of Gantrez particles has several limitations. The formation of aggregates is evident in **Figure 4.2**(A). This phenomenon is usually due to the fact that the colloidal suspension is not stable enough (e.g. the surface charge is low) and that, in this case, could have happened because not enough HA polymer existed to cover the particles, meaning several of them had reminiscent positive charge from the AC, which induce aggregation. Therefore, they are in Regime I when it comes to the HA layer depositions, were low HA concentration was added to a relatively high amount of particles in solution (colloids > polyelectrolytes)[40].

In **Figure 4.2**(B), the image suggests a better LbL build-up on the particles up until the 4th Layer. Although that they seem that way, the results obtained through DLS and Fluorescence Spectroscopy, show that this was not the case (although, of course, there are for sure a number of particles that have been able to succeed in the envelopment of a few layers), and it is probably a case of complexation of HA with AC at a lower scale than the Control (**Figure 4.1**) previously shown.

Figure 4.3 shows an even clearer case of a simple AC/HA complex formed (a lot of these could be visualized on the fluorescence microscope throughout the sample). This leaded to the exclusion of this sample due to the fouling of the membrane.

It is also possible to see in every picture a green background, which indicates a great amount of free FITC labeled, reinforcing the idea that there are a lot of complexes formed.

4.3.2 Characterization using Fluorescence Spectroscopy

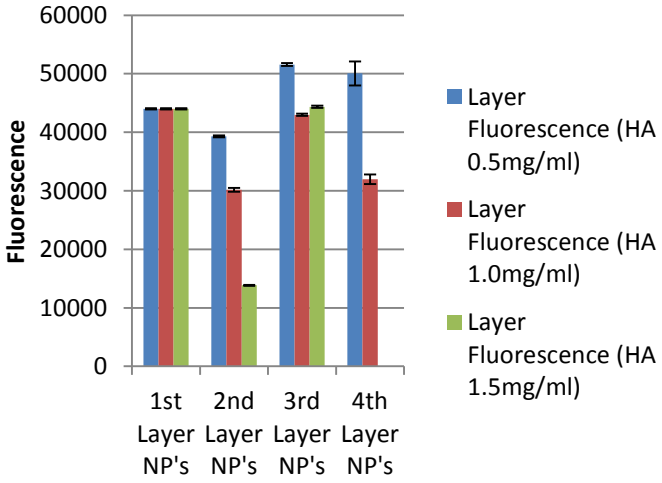

Figure 4.4 - Particle Fluorescence, measured at a gain of 69 for every layer.

Theoretically, the layers with AC, should have higher fluorescence signal, due to the presence of FITC. While the HA layers should have a blinding effect, lowering considerably the signal. Also, the signal in each AC layer should get bigger and bigger, as the particles have more AC surrounding them.

But, in these results, the only clear case of that event, is on the difference between the 1st and 3rd Layers of AC in the HA (0.5mg/ml) sample, where there's an increase of around 5000 fluorescence units. In the other samples (with different HA concentrations), probably due to the low molecular weight of the HA, there is little coverage of the NPs by this polymer, and, consequently, it wasn't possible to compensate the AC charge of the 1st Layer. Meaning that the 3rd Layer (AC deposition), didn't have surface of HA to connect to. This suggests a poor layering capacity through this method. But more evidence follows next with the DLS technique.

Characterization using Dynamic Light Scattering

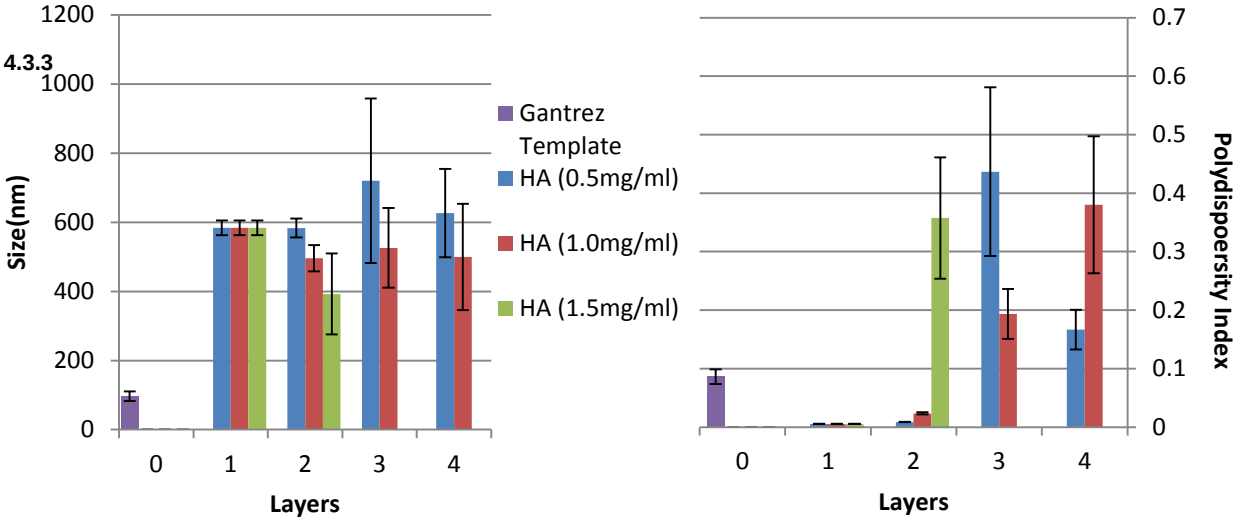

Figure 4.5 - Particle size variation with the addition of successive layers on the left, and on the right graph, PDI variation with same addition of layers

Note: The 1st Layer has the same value for every sample because they started from the same sample of AC.

The results from the DLS support the previous obtained results of a possible poor layering. The expected behavior of layer addition is to get bigger with AC/HA additions but the AC/HA interactions cause the structure to become more compact[48], becoming smaller particle structures. This way an up-down-up variation with the addition of the different layers is expected. Again, the only clear case of this is on the HA (0.5mg/ml) sample, and even there, when the 2nd Layer was added, not much difference was seen, which suggests a poor layering from the start.

Main Conclusions

This method is clearly flawed, being the main problem, the difficulties in purifying the particles after each layer addition, leading to a high amount of free AC-FITC (proved by the high backgroung signal measured through fluorescence and seen on the microscope, showing a slightly green background), which is bad due to the fact that, when HA was added to this mix, instead of interacting exclusively with the particles, it also complexates with the free AC-FITC, creating large complexes of these to polyelectrolytes, contributing to the membrane fouling. So, even though the particles may have been able to form the layers around them, the amount of other complexes made form the two polymers result in bigger size particles with high polydispersity index (complexes). Therefore, other methods for washing after each layer deposition have to be used.

4.4 Characterization of AC/HA LbL Nanoparticles obtained by Ultracentrifugation

This type of centrifuge works on high vacuum conditions, and therefore requires only a small amount of driving energy while attaining very high rotation speeds.

For this experiment, the particles were separated in 3 different samples, differing only in the concentration of particles, which were $1.98x10^{12}$NP/ml, $9.9x10^{11}$NP/ml and $4.95x10^{11}$ NP/ml, corresponding to samples diluted 2000x, 4000x and 8000x, respectively.

Note: In order to ease the reading, particle concentrations will be referred to by their dilution instead of concentration.

4.4.1 Zeta Potential

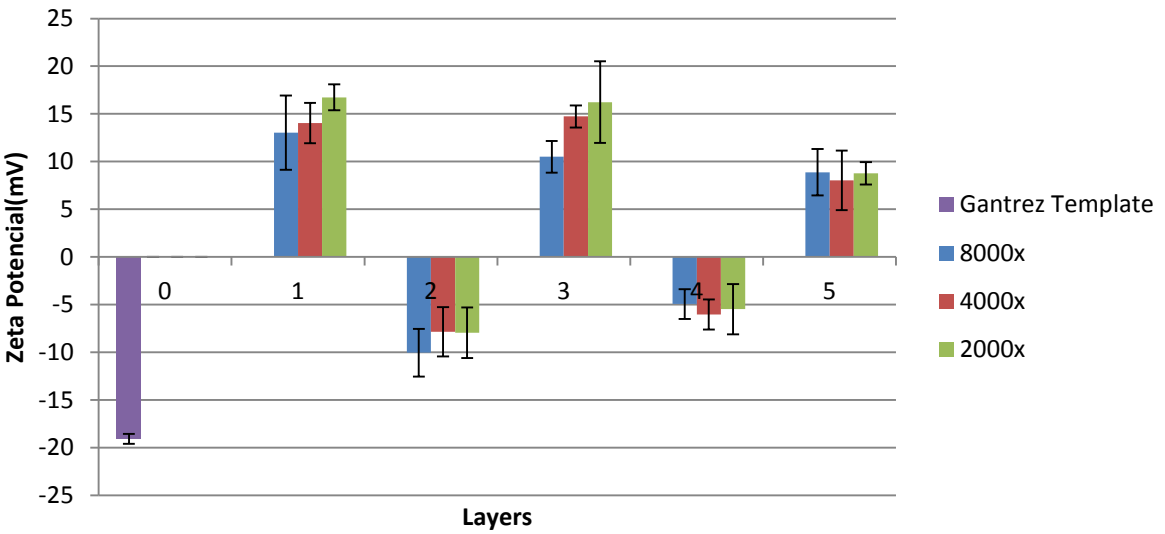

Figure 4.6 - Zeta Potencial variation for the different layers added.

Knowing that the Aminocelulose and the Hyaluronic Acid have positive, and negative charge, respectively, and that the AC is the first one to be deposited followed by HA, alternating successively between them, the variation of the ZP of the particles in solution proves layers deposition. That can be explained by the fact that the polymer that is attached to the particles in each deposition, coat the particles, becoming the outer layer, giving off a signal (positive or negative) with the similar charge as the polymer deposited.

Now, comparing the different dilutions used, only through ZP analysis, it's not possible to decide which one gives us the best results as the values don't differ that much between them.

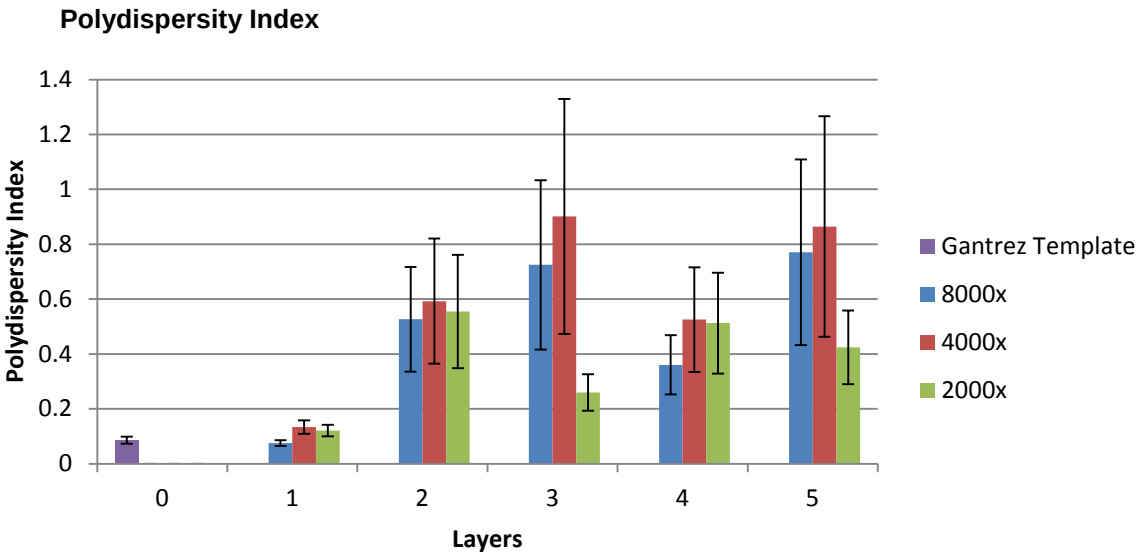

Figure 4.7 - Polydispersity variation gor the different layer depositions.

The PDI was measured using the DLS technique, allowing us to understand the distribution profile of the particles in solution in every step of layer deposition. The results allow us to study effect of particles concentrations on the suspension stability in order to obtain NPs with a low PDI. An increase in PDI indicates larger range of particle size in solution.

Analysing these results, it's fair to say that the particles that show the best deposition profile should be the 2000x diluted, as their PDI never goes over 0.6, while the other ones do. It is recommended, for the DLS technique, that the PDI stays lower than 0.6-0.7, as values bigger than those promote a higher reading error and they're not recommended for DLS reading[49].

4.4.3 Particle Size Variation

For this analysis, two methods were used. The Dynamic Light Scattering technique again, and Nanoparticle Tracking Analysis. The first was used to follow the layering process, while the latter was only used on the final 5th Layer, in order to verify the particle size.

Although we have both analyses it is evident through the previous PDI results, that we have a polydisperse sample. Being that the case, the NTA provides results more reliable when compared to DLS, because the NTA has a particle-by-particle approach which allows a better resolution of NP's sizes and there's no intensity bias towards larger particles. The DLS isn't as good for polydisperse analysis because average particle size is intensity biased towards the larger/contaminant particles within a sample[47].

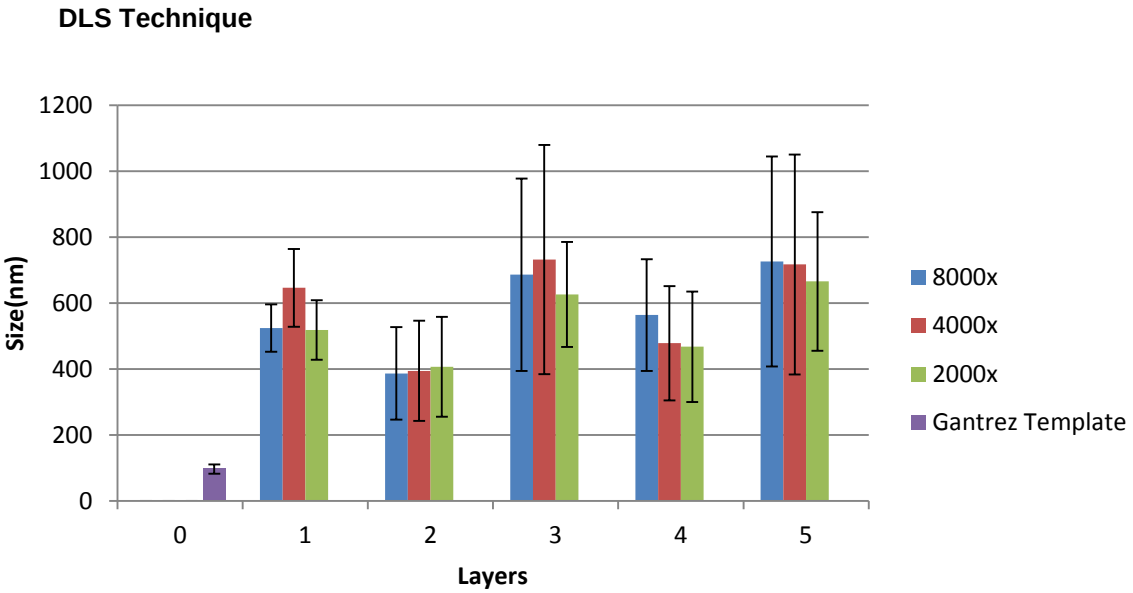

Figure 4.8 - Size variation with the different layer depositions.

These results show a positive difference in the layering of the NP's, when compared to the filter units method. The big difference here was that the particles were able to be purified after each polymer addition, allowing the next polymer added to coat the particles, and no AC/HA complexes where formed.

The particle size variation was the expected for every dilution, except maybe for the 4000x sample, where from the 3rd to the 5th layer there was a decrease of the average size value of around 15 nm.

NTA Technique

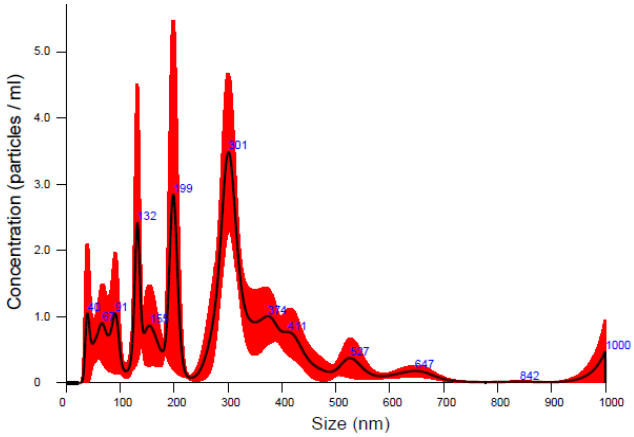

Figure 4.9 - NPs Concentrations for different sizes for the 9.9x10^{11} NP/ml sample

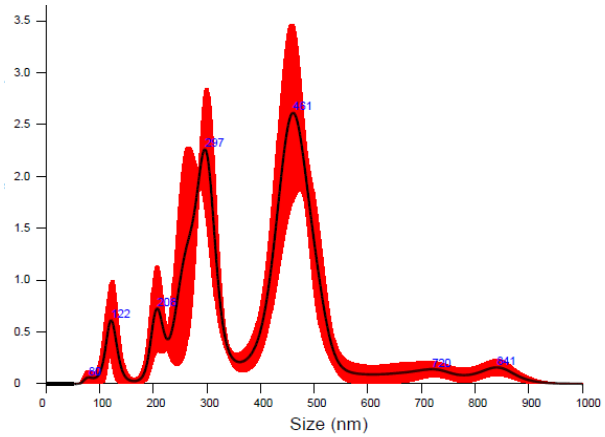

Figure 4.10 - NPs Concentrations for different sizes for the 1.98x10^{12} NP/ml sample

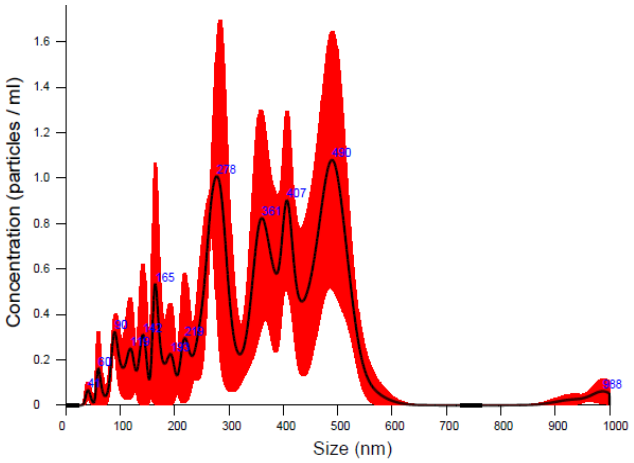

Figure 4.11 - NPs Concentrations for different sizes for the 4.95x10^{11} NP/ml sample

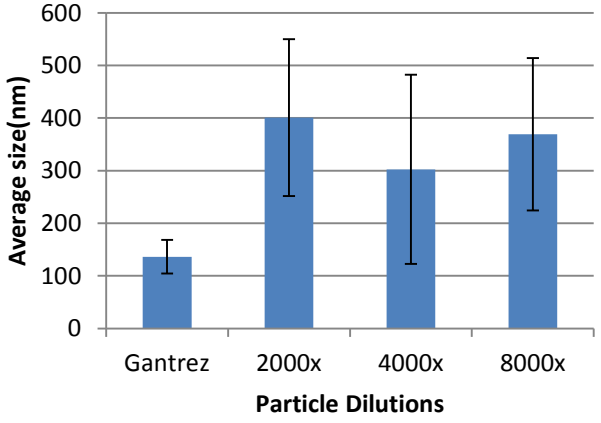

Figure 4.12 – Particle size variation after 5 layer depositions for the different dillutions. Gantrez is without any layer

The graphs back up the PDI values previously shown. It is clear the existence of different particle concentration peaks for different particle sizes, proving that we do have polydisperse samples in all cases and that the 2000x diluted is the less polydisperse, as it has less variety of different sized particles.

On the Figure 2.12, the value that differs most from the others is the one for the 4000x sample. This may be due to the not so good layering in these particles, corroborating the results previously shown in the Figure 2.8 with the size variation, showing that the size didn't get bigger, like what happened with the other samples, and stayed with a final size a little lower. Although this happened, it is strange that the 2000x and 8000x managed to layer correctly, while the 4000x didn't. So, probably a practical error was the cause.

Table 4-2 - Concentration of NPs after layering, obtained through NTA and calculated to the point of 0x dilution for each sample. Yield was also calculated and displayed in percentage.

Sample	Gantrez	2000x	4000x	8000x
NP/ml	3.96E+15	4.53E+13	4.81E+13	2.47E+13
Yield(%)	(no yield as this is the starting concentration)	1.143939	1.214646	0.623737

A low yield was expected due to the ultracentrifugation. There have been reports that, for Gold NPs yields of around 80% for each washing step were attained[50], so in that case, 5 washing steps would lead to $0.8^5 = 0.32$, or 32% yield. This value is higher than what we had, but it is important to mention that it was the first time these polymers were used for this kind of process, so it is not yet fully optimized. Also, after every layer deposition, several measurements were performed (DLS, ZP and on the 5th Layer NTA was also made), and inevitably some particles are lost in the measurements.

4.4.4 Main Conclusions

Through the Ultracentrifugation method, it is possible to create and purify Layer-by-Layer polyelectrolyte Nanoparticles, at least up to 5 layers. Although the final sample is polydisperse, through NTA and Laser Doppler Micro-electrophoresis it is still possible to characterize most of the particle properties with confidence.

4.5 Antibacterial Effect

Knowing that the AC has an antibacterial effect, and that bacteria are capable of producing enzymes capable of degrading Hyaluronic Acid, the particles could have the AC released and produce an antibacterial effect. To observe the antibacterial capacity of the assembled particles, tests were made.

Firstly, the antibacterial capacity of the Aminocelulose was observed, and the results obtained were as follows:

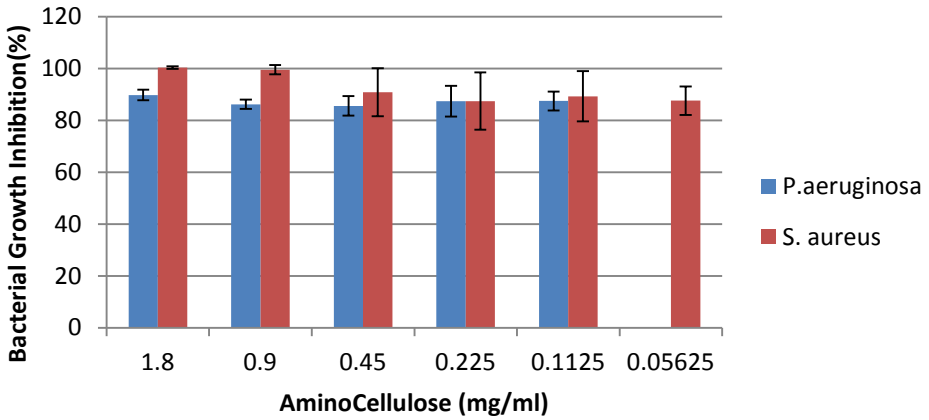

Figure 4.13 - Aminocellulose Antibacterial test results

The experiment showed that the aminocellulose has an overall high antibacterial effect, for either gram-positive (*S. aureus*) or gram-negative (*P. aeruginosa*) bacteria. But for the gram-negative bacteria, growth isn't inhibited at all in concentrations lower than 0.05625mg/ml, while in the gram-positive, there is still significant antibacterial effect on the same concentration.

The same protocol was followed for all of the different particles made

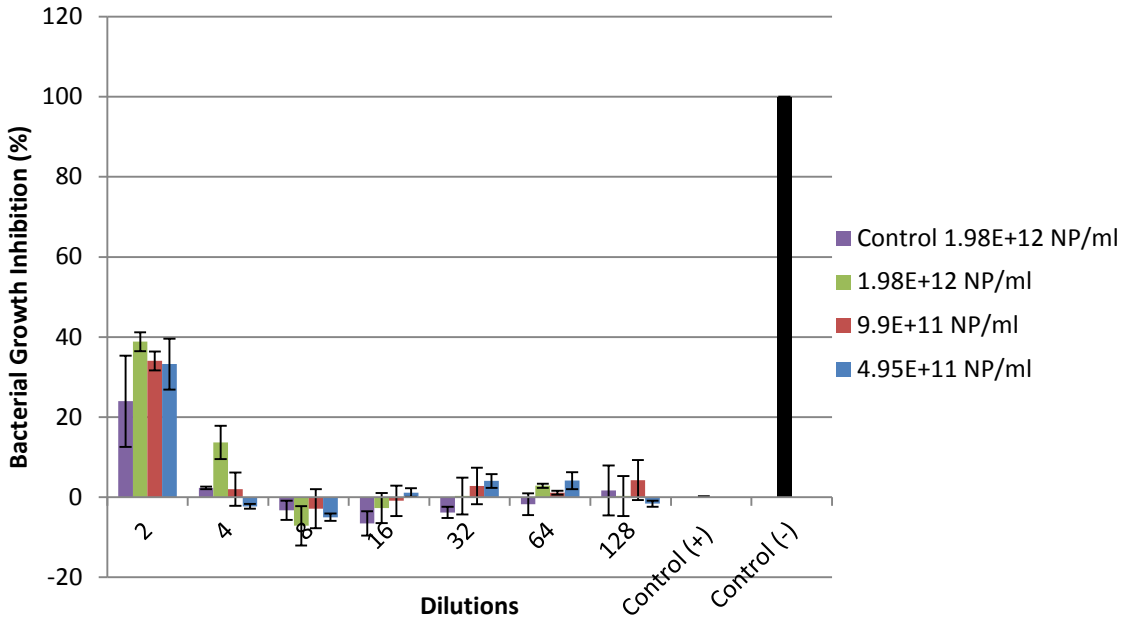

Figure 4.14 - NPs LbL antibacterial test on S. aureus results serially diluted up to 128 times. Control (-)was 75µl Gentamycin (100µg/ml) + 75µl bacteria (OD=0.01) and the Control (+) was 75µl MH + 75µl bacteria (OD=0.01)

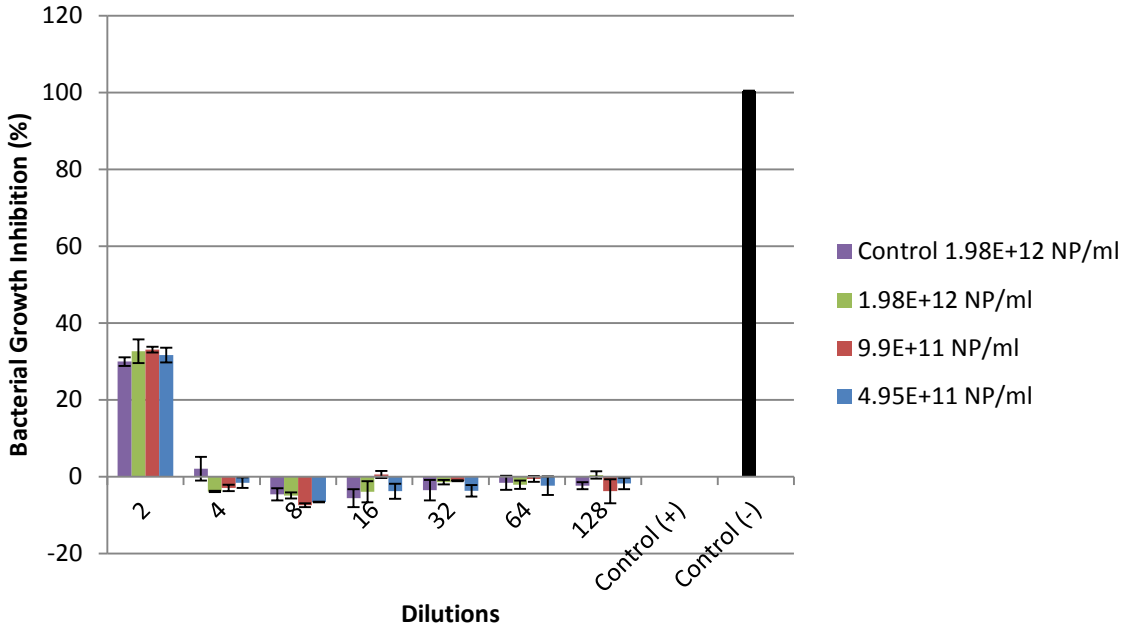

Figure 4.15 - NPs LbL antibacterial test on P. aeruginosa results serially diluted up to 128 times. Control (-)was 75µl Gentamycin (100µg/ml) + 75µl bacteria (OD=0.01) and the Control (+) was 75µl MH + 75µl bacteria (OD=0.01)

Although it was previously proved that the aminocellulose had high antimicrobial activity, it is plain to see that that the particles do not show any kind of antibacterial effect, nor for the gram-positive bacteria and neither for the gram-negative bacteria. The only one that shows any sign of it is the 2x dilution, but that can be explained due to the pH used (4.5), which is the same for all the dilutions and gantrez template. As acid pH has antimicrobial properties, that dilution shows some effect (as it is the less diluted sample), but it can't be attributed to the particles and this is the reason all of the samples show the same behavior in every dilution.

The weak (or inexistent) antimicrobial power can be explained by a few factors.

Firstly, the starting work concentrations were already really low (8000x, 4000x, 2000x dilutions), and besides, the yield of the whole process reduces the number of particles to around 1% of the original particle concentration. This low concentration of particles also means a low concentration of amino cellulose, which is the only component with antibacterial activity in the samples. It was previously shown in **Figure 4.13** that there is no bacterial growth inhibition in cases of low concentrations of AC, which is certainly this case.

Secondly, the number of layers is only 5, from which only 3 correspond to amino cellulose layers, which gives us a very low amount of AC around each particle. As a consequence, there is very little antibacterial effect around each LbL NP.

These two factors indicate very low amounts of AC in the media, explaining why the antibacterial tests failed.

4.6 Lactonase Cloning, Expression, Purification

Lactonase Dna Amplification

4.6.1 pET22b vector containing the lactonase gene was amplified by following the Miniprep protocol (Appendix7.1). Upon DNA purification, a UV-spectrum was run in order to determine DNA concentration and purity.

Table 4-3 - Spectroscopic characterization of the lactonase containing vector upon DNA amplification. CorrAbs corresponds to the absorbance corrected by removal of the baseline for both 260nm and 280nm wavelengths, respectively. DF stands for the dilution factor (1/60) [C] is the final concentration considering that one Optical density value is equivalent to 50µg/ml, and 260/280 is the ratio between both absorbances to determine the purity of the sample.

Sample	$corrAbs_{(260nm)}$	$corrAbs_{(280nm)}$	$DF*[C]_{260}$(µg/ml)	$DF*[C]_{280}$(µg/ml)	260/280
A	0.0377	0.0182	113.1	54.6	2.071429
B	0.0312	0.0194	93.6	58.2	1.608247
C	0.0571	0.0295	171.3	88.5	1.935593

Through the analysis of this table, it is safe to assume that the best DNA to use was from sample C. Not only it had a lot more DNA concentration, but it also was the one that ratio 260/280 was optimal, between 1.8 and 2.0. This means that the amounts of RNA, contributing to A260nm, and protein, at A280nm, were really low being the DNA almost pure.

Optimization of Lactonase Expression through IPTG induction

Several IPTG concentrations were tested in order to optimize Lactonase expression.

4.6.2

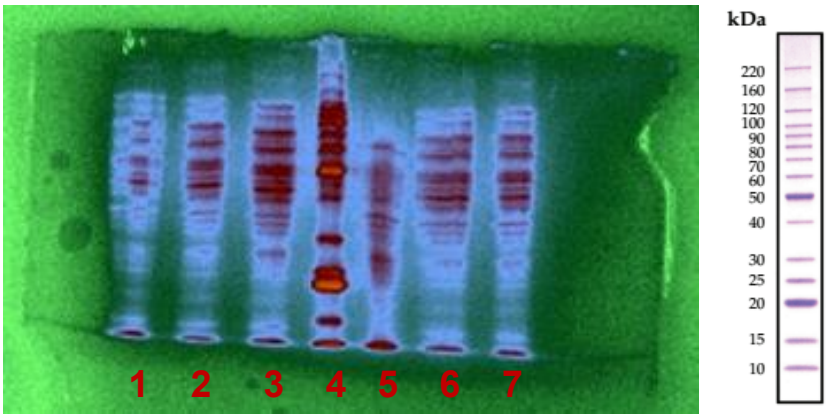

Figure 4.16 – SDS-Page results for the expression of the Lactonase in E. Coli BL21 (DE3) under different concentrations of IPTG. Lane 1,2,3,5,6 and 7 were samples induced with 0, 0.1, 0.2, 0.4, 0.8 and 1 mM IPTG, respectively. The molecular weight marker was run in lane 4. The set of protein standards used to identify the approximate size of lactonase are shown on the right.

The only lane that shows a stronger band at around 28kDa, corresponding to the molecular weight of Lactonase [51], is 3, suggesting 0.2 mM IPTG the best conditions for lactonase expression. However, Coomassie staining dyes all the protein content, so another technique is needed in order to specifically confirm that band as lactonase. For this purpose, a Western Blot using an antibody specific for the 6xHisTag was carried out.

Figure 4.17 – Western Blot results for the expression of the Lactonase in . *E. Coli* BL21 (DE3) under different concentrations induction with IPTG

Western-blot results confirm the conclusions obtained from the SDS-PAGE, being 0.2 mM the best IPTG concentration for expression. Moreover, this very sensitive technique also detects lactonase when using 0.1 and 0.4mM IPTG, not easy to observe by Coomassie blue staining.

4.6.3 Lactonase Purification

Having verified Lactonase expression, the purification procedure was followed, and for every step, a small sample was loaded to a SDS-PAGE. In parallel, a gel was prepared with 4 different amounts (in µg) of albumin, the final eluent and molecular weight marker in order to know the approximate lactonase amount obtained.

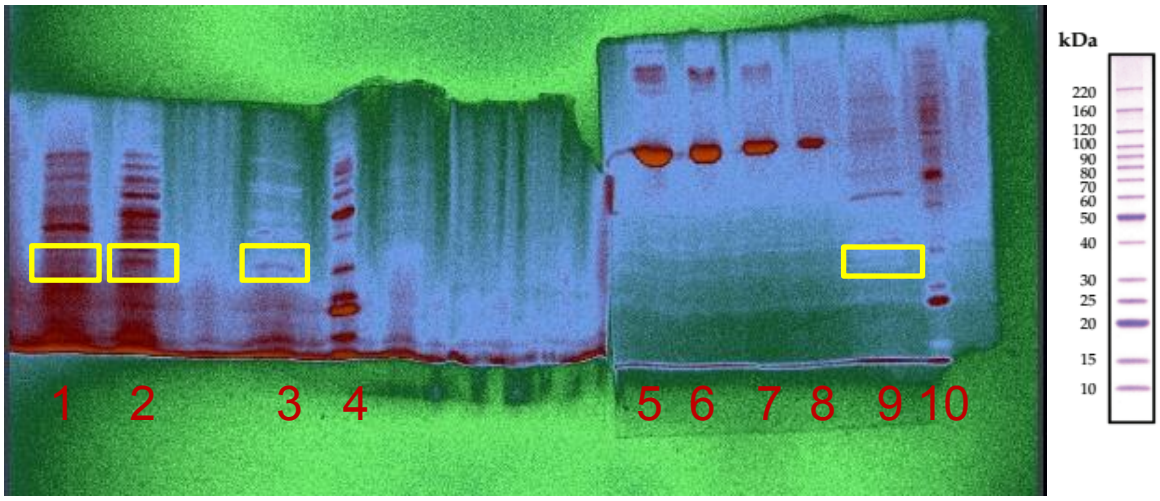

Figure 4.18 - SDS-PAGE gels containing samples from Lactonase purification protocol. On the left, samples collected during the Lactonase purification procedure. On the right, comparison between different amounts of albumin (in µg) with purified sample. Lanes: 1-Sample FT, 2- FT from the wash step, 3 and 9- Eluted sample, 4 and 10- Molecular weight Marker; 5, 6, 7 and 8 correspond to 0.75µg, 0.5µg, 0.25µg 0.1µg of albumin. Yellow boxes highlight the band corresponding to lactonase. Marker scale is on the furthest right for better comprehension.

Analysing the gels, it is possible to see that there is probably lactonase, at least in the sample lane 2, corresponding to the wash step. However, it is very hard to observe lactonase in the other lanes. Lane 3, corresponding to the eluted protein, presents only a slight band around 30KDa suggesting that the protein was lost in the washing steps. This is probably due to the concentration of Imidazole used for washing, leading to protein elution in this step.

This way, a new purification was carried out, but this time with an Imidazole gradient, in order to ascertain where the protein of interest was lost. Note that the protocol was repeated from the transformation step. The result was as follows:

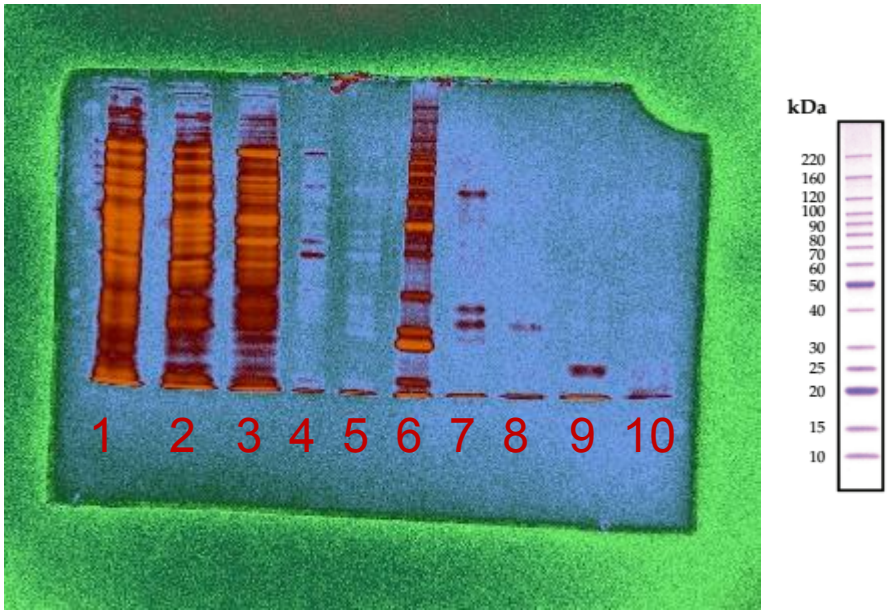

Figure 4.19: SDS-PAGE results for the Purification of Lactonase using different concentrations of Imidazole in the washing steps. Lanes: 1-Initial Sample, 2-Sample FT, 3,4,5,7,8,9- Washing steps using 50, 100, 150, 200, 250 and 300mM Imidazole, respectively, 6-Molecular weight Marker, 10-Elution (in 500mM Imidazole). Information about the protein standards size is on the right for better comprehension.

On the 7th and 8th lanes, it is possible to see bands around the 30kDa size, possibly being the lactonase. Western blot results that followed did not show any band, indicating lack of lactonase, so, after trying new cells with fresh media, and still no results, the only problem possible was that the original DNA containing the gene had some kind of problem.

This issue was addressed by running an agarose gel electrophoresis with the 3 DNA samples, A, B and C.

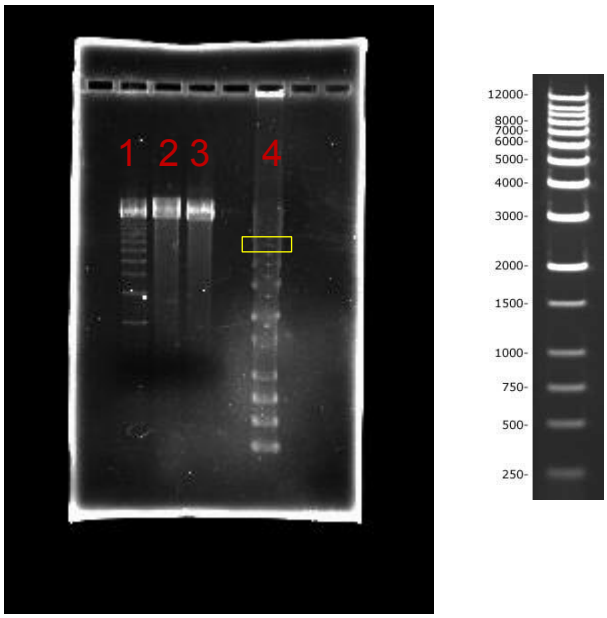

Figure 4.20 - DNA Electrophoresis results. Tracks: 1, 2 and 3 - A, B and C, respectively; 4 – Molecular weigh Marker. Yellow box highlights the 6000 base pair (bp) band, the lactonase containing vector size, for clarity. On the right is the marker with the respective size of each band in bp.

As it is possible to see, there is clearly something wrong with the DNA, showing little progression on the gel, when it should have run until 6 Kbp, yellow box. Also, in lane 1, there's a clear sign of DNA fragmentation being in lanes 2 and 3 more a degradation pattern. This way, it was impossible to keep on producing lactonase through this method with this DNA. A new DNA was amplified and purified, but unfortunately, it was impossible to do the same method with the new DNA while the internship lasted

4.6.4 Optimization of Lactonase Expression and Purification by using autoinducing media

Another protocol was followed, the Auto-Induction Protocol, to avoid the step of IPTG induction, allowing the lactonase to be produced by the bacteria through the use of a special media containing lactose.

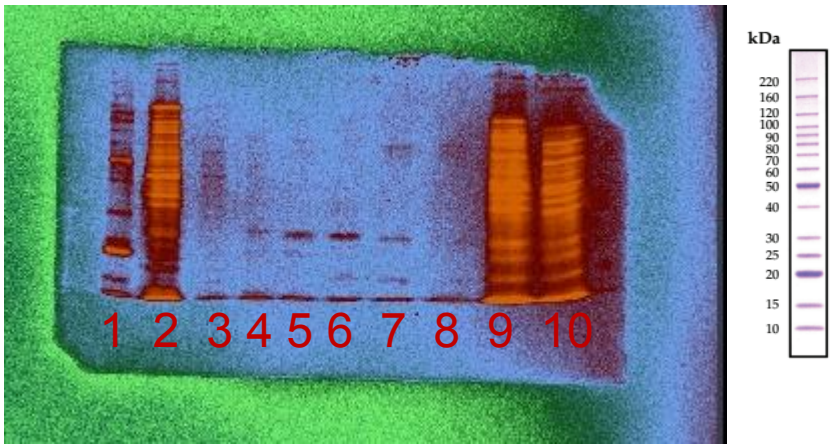

Figure 4.21 SDS-PAGE results for the Purification of the Lactonase through Auto-Induction in E. Coli BL21 (DE3). Lane 1- Molecular weight marker; 2,3,4,5,6,7 - Washing steps using 50, 100, 150, 200, 250 and 300mM Imidazole, respectively; 8-Eluted protein (at 500mM Imidazole); 9-Initial Sample; 10-Sample FT. Standard protein size are on the right for better comprehension.

After purification (through the use of the gradient again), the lanes that showed the best results were the 5th and the 6th, showing evident bands around the 30kDa, After this, another Western blot was carried out.

Figure 4.22 – On the upper part, SDS-PAGE results for the Purification of the Lactonase using autoinducing media in E. Coli BL21 (DE3). Below, the corresponding Western Blot. Marker is on the right for better comprehension. Lanes: 1-Initial Sample, 2-Sample FT, 3,4,5,7,8,9- Washing steps using 50, 100, 150, 200, 250 and 300mM Imidazole, respectively, 6-Molecular Weight Marker, 10-Eluted protein (in 500mM Imidazole).

The Western blot indicates that there is lactonase in lanes 5, 6 and 7, corresponding to concentrations of imidazole of 250mM, 300mM and 500mM, respectively.

4.6.5

Main Conclusions

Although the purification through IPTG induction wasn't possible due to DNA fragmentation, it was still possible to produce lactonase in the first experiments through that method. So, it is not a protocol to be discarded, it just has remade once a new lactonase DNA is available.

But, the autoinducing media protocol showed promising results in producing lactonase. The newly amplified DNA was used for this method, and after purification, it was possible to ascertain that the elution of lactonase starts at a concentration of around 250mM Imidazole

5 Future Work

Even though the production of the LbL Nanoparticles was accomplished, several improvements still have to be made to the protocol. Particle concentration should be higher, and, in order to accomplish that, the protocol made should be repeated for different higher concentrations. This would help understand, in these conditions, what is the maximum concentration of particles which is possible to work with, still allowing good polyelectrolyte deposition and small levels of aggregation. Besides, the centrifugation yield is very low, giving even lower final particle concentrations than expected. This can be raised by optimizing centrifugation times, as usually, with more prolonged centrifugation times, a higher yield is obtained[52]. After maximum NP concentration and ideal centrifugation time are assessed, the next step would be working on having more layers, to improve the particle antibacterial property.

Regarding the lactonase production and purification, production was shown to be possible through both protocols used, and the purification protocol also worked. But, in the purification, the next step needs to be accomplished in the near future. Which means, knowing that the lactonase elutes above 250mM Imidazole concentrations, a real purification has to be made, obtaining a purified solution of lactonase, able to be used for future experiments. And also, produce higher amounts of it, by growing larger volumes of bacterial suspensions that are able to express this enzyme.

When the particle and lactonase productions are finely tuned, the next phase will start. Here, hybrid LbL particles will be produced. The lactonase would be incorporated in the particles as one of the layers. This is theoretically possible as the lactonase is positively charged below its isoelectric point of 4.7 [53], and the pH used for the LbL experiment is 4.5 (This pH may need to be lowered for the lactonase incorporation, as it may not provide enough positive charge on the enzyme).

Hopefully after all this, a new hybrid NP system will be obtained with high antimicrobial activity, while maintaining its non-toxic properties against human cells, making it possible to apply on the skin through future cream and lotion formulations.

6 References

[1] V. Ki and C. Rotstein, “Bacterial skin and soft tissue infections in adults: A review of their epidemiology, pathogenesis, diagnosis, treatment and site of care,” *Can. J. Infect. Dis. Med. Microbiol.*, vol. 19, no. 2, pp. 173–184, Mar. 2008.

[2] R. I. Aminov, “A Brief History of the Antibiotic Era: Lessons Learned and Challenges for the Future,” *Front. Microbiol.*, vol. 1, Dec. 2010.

[3] “European Medicines Agency - News and Events - The bacterial challenge - Time to react a call to narrow the gap between multidrug-resistant bacteria in the EU and development of new antibacterial agents.” [Online]. Available: http://www.ema.europa.eu/ema/index.jsp?curl=pages/news_and_events/news/2009/11/news_detail_000044.jsp&mid=WC0b01ac058004d5c1. [Accessed: 26-Sep-2016].

[4] R. I. Aminov and R. I. Mackie, “Evolution and ecology of antibiotic resistance genes,” *FEMS Microbiol. Lett.*, vol. 271, no. 2, pp. 147–161, Jun. 2007.

[5] K. D. Koirala, “Antibiotic Resistance and the Future,” *JAMA*, vol. 305, no. 22, p. 2293, Jun. 2011.

[6] P. M. Bennett, “Plasmid encoded antibiotic resistance: acquisition and transfer of antibiotic resistance genes in bacteria,” *Br. J. Pharmacol.*, vol. 153, no. Suppl 1, pp. S347–S357, Mar. 2008.

[7] M. B. Miller and and B. L. Bassler, “Quorum Sensing in Bacteria,” *Annu. Rev. Microbiol.*, vol. 55, no. 1, pp. 165–199, 2001.

[8] Y.-H. Dong, L.-H. Wang, and L.-H. Zhang, “Quorum-quenching microbial infections: mechanisms and implications,” *Philos. Trans. R. Soc. B Biol. Sci.*, vol. 362, no. 1483, pp. 1201–1211, Jul. 2007.

[9] F. Chen, Y. Gao, X. Chen, Z. Yu, and X. Li, “Quorum Quenching Enzymes and Their Application in Degrading Signal Molecules to Block Quorum Sensing-Dependent Infection,” *Int. J. Mol. Sci.*, vol. 14, no. 9, pp. 17477–17500, Aug. 2013.

[10] B. Thallinger *et al.*, “Cellobiose dehydrogenase functionalized urinary catheter as novel antibiofilm system,” *J. Biomed. Mater. Res. B Appl. Biomater.*, vol. 104, no. 7, pp. 1448–1456, Oct. 2016.

[11] K. Ivanova *et al.*, “Quorum-Quenching and Matrix-Degrading Enzymes in Multilayer Coatings Synergistically Prevent Bacterial Biofilm Formation on Urinary Catheters,” *ACS Appl. Mater. Interfaces*, vol. 7, no. 49, pp. 27066–27077, Dec. 2015.

[12] M. Yasuyuki, K. Kunihiro, S. Kurissery, N. Kanavillil, Y. Sato, and Y. Kikuchi, “Antibacterial properties of nine pure metals: a laboratory study using Staphylococcus aureus and Escherichia coli,” *Biofouling*, vol. 26, no. 7, pp. 851–858, Oct. 2010.

[13] A. Jain, L. S. Duvvuri, S. Farah, N. Beyth, A. J. Domb, and W. Khan, “Antimicrobial Polymers,” *Adv. Healthc. Mater.*, vol. 3, no. 12, pp. 1969–1985, Dec. 2014.

[14] N. Beyth, Y. Houri-Haddad, A. Domb, W. Khan, and R. Hazan, “Alternative Antimicrobial Approach: Nano-Antimicrobial Materials,” *Evid. Based Complement. Alternat. Med.*, vol. 2015, p. e246012, Mar. 2015.

[15] A. Francesko *et al.*, “Bacteria-responsive multilayer coatings comprising polycationic nanospheres for bacteria biofilm prevention on urinary catheters,” *Acta Biomater.*, vol. 33, pp. 203–212, Mar. 2016.

[16] E. A. Grice and J. A. Segre, “The skin microbiome,” *Nat. Rev. Microbiol.*, vol. 9, no. 4, pp. 244–253, Apr. 2011.

[17] S. T. Rutherford and B. L. Bassler, “Bacterial Quorum Sensing: Its Role in Virulence and Possibilities for Its Control,” *Cold Spring Harb. Perspect. Med.*, vol. 2, no. 11, Nov. 2012.

[18] E. G. Ruby, “Lessons from a cooperative, bacterial-animal association: the Vibrio fischeri-Euprymna scolopes light organ symbiosis,” *Annu. Rev. Microbiol.*, vol. 50, pp. 591–624, 1996.

[19] J. W. Hastings and E. P. Greenberg, “Quorum Sensing: the Explanation of a Curious Phenomenon Reveals a Common Characteristic of Bacteria,” *J. Bacteriol.*, vol. 181, no. 9, pp. 2667–2668, May 1999.

[20] V. C. Kalia, *Quorum Sensing vs Quorum Quenching: A Battle with No End in Sight*. Springer, 2014.

[21] K. B. Xavier and B. L. Bassler, “Interference with AI-2-mediated bacterial cell-cell communication,” *Nature*, vol. 437, no. 7059, pp. 750–753, Sep. 2005.

[22] J. M. Rothfork *et al.*, “Inactivation of a bacterial virulence pheromone by phagocyte-derived oxidants: new role for the NADPH oxidase in host defense,” *Proc. Natl. Acad. Sci. U. S. A.*, vol. 101, no. 38, pp. 13867–13872, Sep. 2004.

[23] K. Ivanova, M. M. Fernandes, E. Mendoza, and T. Tzanov, “Enzyme multilayer coatings inhibit Pseudomonas aeruginosa biofilm formation on urinary catheters,” *Appl. Microbiol. Biotechnol.*, vol. 99, no. 10, pp. 4373–4385, May 2015.

[24] S. Fetzner, “Quorum quenching enzymes,” *J. Biotechnol.*, vol. 201, pp. 2–14, May 2015.

[25] C. Reimmann *et al.*, “Genetically programmed autoinducer destruction reduces virulence gene expression and swarming motility in Pseudomonas aeruginosa PAO1,” *Microbiol. Read. Engl.*, vol. 148, no. Pt 4, pp. 923–932, Apr. 2002.
[26] S. J. Lee, S.-Y. Park, J.-J. Lee, D.-Y. Yum, B.-T. Koo, and J.-K. Lee, “Genes encoding the N-acyl homoserine lactone-degrading enzyme are widespread in many subspecies of Bacillus thuringiensis,” *Appl. Environ. Microbiol.*, vol. 68, no. 8, pp. 3919–3924, Aug. 2002.
[27] M. Singh, S. Singh, S. Prasad, and I. S.gambhir, “Nanotechnology in medicine and antibacterial effect of silver nanoparticles,” *ResearchGate*, vol. 3, no. 3, pp. 115–122, Sep. 2008.
[28] R. Y. Pelgrift and A. J. Friedman, “Nanotechnology as a therapeutic tool to combat microbial resistance,” *Adv. Drug Deliv. Rev.*, vol. 65, no. 13–14, pp. 1803–1815, Nov. 2013.
[29] C. Wiegand, M. Nikolajski, U.-C. Hipler, and T. Heinze, “Nanoparticle Formulation of AEA and BAEA Cellulose Carbamates Increases Biocompatibility and Antimicrobial Activity,” *Macromol. Biosci.*, vol. 15, no. 9, pp. 1242–1251, Sep. 2015.
[30] A. Francesko *et al.*, “Enzymatic functionalization of cork surface with antimicrobial hybrid biopolymer/silver nanoparticles,” *ACS Appl. Mater. Interfaces*, vol. 7, no. 18, pp. 9792–9799, May 2015.
[31]J. J. Kirkland, “Porous Thin-Layer Modified Glass Bead Supports for Gas Liquid Chromatography.,” *Anal. Chem.*, vol. 37, no. 12, pp. 1458–1461, Nov. 1965.
[32] G. Decher and J.-D. Hong, “Buildup of ultrathin multilayer films by a self-assembly process, 1 consecutive adsorption of anionic and cationic bipolar amphiphiles on charged surfaces,” *Makromol. Chem. Macromol. Symp.*, vol. 46, no. 1, pp. 321–327, Jun. 1991.
[33] M. Lotfi, M. Naceur, and M. Nejib, *Cell Adhesion to Biomaterials: Concept of Biocompatibility*. INTECH Open Access Publisher, 2013.
[34] I. Zhuk, F. Jariwala, A. B. Attygalle, Y. Wu, M. R. Libera, and S. A. Sukhishvili, “Self-defensive layer-by-layer films with bacteria-triggered antibiotic release,” *ACS Nano*, vol. 8, no. 8, pp. 7733–7745, Aug. 2014.
[35] B. Zhou, Y. Li, H. Deng, Y. Hu, and B. Li, “Antibacterial multilayer films fabricated by layer-by-layer immobilizing lysozyme and gold nanoparticles on nanofibers,” *Colloids Surf. B Biointerfaces*, vol. 116, pp. 432–438, Apr. 2014.
[36] P. R. Gil, L. L. del Mercato, P. del_Pino, A. Muñoz_Javier, and W. J. Parak, “Nanoparticle-modified polyelectrolyte capsules,” *Nano Today*, vol. 3, no. 3–4, pp. 12–21, Jun. 2008.
[37] Y. Wu *et al.*, “Layer-by-Layer (LBL) Self-Assembled Biohybrid Nanomaterials for Efficient Antibacterial Applications,” *ACS Appl. Mater. Interfaces*, vol. 7, no. 31, pp. 17255–17263, Aug. 2015.
[38] P. Jain, S. Jain, K. N. Prasad, S. K. Jain, and S. P. Vyas, “Polyelectrolyte Coated Multilayered Liposomes (Nanocapsules) for the Treatment of Helicobacter pylori Infection,” *Mol. Pharm.*, vol. 6, no. 2, pp. 593–603, Apr. 2009.
[39] K. Rahn, M. Diamantoglou, D. Klemm, H. Berghmans, and T. Heinze, “Homogeneous synthesis of cellulose p-toluenesulfonates in N,N-dimethylacetamide/LiCl solvent system,” *Angew. Makromol. Chem.*, vol. 238, no. 1, pp. 143–163, Jun. 1996.
[40] G. Schneider and G. Decher, “Functional core/shell nanoparticles via layer-by-layer assembly. investigation of the experimental parameters for controlling particle aggregation and for enhancing dispersion stability,” *Langmuir ACS J. Surf. Colloids*, vol. 24, no. 5, pp. 1778–1789, Mar. 2008.
[41] “Zetasizer Nano user manual (English).” [Online]. Available: http://www.malvern.com/en/support/resource-center/user-manuals/MAN0485EN.aspx. [Accessed: 30-Oct-2016].
[42] C. G. Malmberg and A. A. Maryott, *Dielectric constant of water from 0° to 100° C*. National Bureau of Standards, 1956.
[43] J. Kestin, M. Sokolov, and W. A. Wakeham, “Viscosity of liquid water in the range −8 °C to 150 °C,” *J. Phys. Chem. Ref. Data*, vol. 7, no. 3, pp. 941–948, Jul. 1978.
[44] “Investigations on the Theory of the Brownian Movement.” [Online]. Available: http://store.doverpublications.com/0486603040.html. [Accessed: 11-Oct-2016].
[45] “Dynamic Light Scattering: An Introduction in 30 Minutes.” [Online]. Available: http://www.malvern.com/en/support/resource-center/technical-notes/TN101104DynamicLightScatteringIntroduction.aspx. [Accessed: 11-Oct-2016].
[46] A. Malloy, “Count, size and visualize nanoparticles,” *Mater. Today*, vol. 14, no. 4, pp. 170–173, Apr. 2011.
[47] “NanoParticle Tracking Analysis (NTA) and Dynamic Light Scattering (DLS) - Comparison between NTA and DLS,” *AZoNano.com*, 21-Jan-2009. [Online]. Available: http://www.azonano.com/article.aspx?ArticleID=2274. [Accessed: 25-Sep-2016].

[48] R. M. A. Domingues *et al.*, “Development of Injectable Hyaluronic Acid/Cellulose Nanocrystals Bionanocomposite Hydrogels for Tissue Engineering Applications,” *Bioconjug. Chem.*, vol. 26, no. 8, pp. 1571–1581, Aug. 2015.
[49] “www.biophysics.bioc.cam.ac.uk - Site Info - Website-Box.net.” [Online]. Available: http://website-box.net/site/www.biophysics.bioc.cam.ac.uk. [Accessed: 30-Oct-2016].
[50] S. K. Balasubramanian, L. Yang, L.-Y. L. Yung, C.-N. Ong, W.-Y. Ong, and L. E. Yu, “Characterization, purification, and stability of gold nanoparticles,” *Biomaterials*, vol. 31, no. 34, pp. 9023–9030, Dec. 2010.
[51] Y.-H. Dong, J.-L. Xu, X.-Z. Li, and L.-H. Zhang, “AiiA, an enzyme that inactivates the acylhomoserine lactone quorum-sensing signal and attenuates the virulence of Erwinia carotovora,” *Proc. Natl. Acad. Sci.*, vol. 97, no. 7, pp. 3526–3531, Mar. 2000.
[52] A. Cvjetkovic, J. Lötvall, and C. Lässer, “The influence of rotor type and centrifugation time on the yield and purity of extracellular vesicles,” *J. Extracell. Vesicles*, vol. 3, Mar. 2014.
[53] L.-H. Wang, L.-X. Weng, Y.-H. Dong, and L.-H. Zhang, “Specificity and Enzyme Kinetics of the Quorum-quenching N-Acyl Homoserine Lactone Lactonase (AHL-lactonase),” *J. Biol. Chem.*, vol. 279, no. 14, pp. 13645–13651, Apr. 2004.

7 Appendix

7.1 MiniPrep Protocol: Plasmid DNA Purification using the QIAprep Spin Miniprep Kit and Microcentrifuge

This protocol is designed for purification of up to 20 µg of high-copy plasmid DNA from 1–5 ml overnight cultures of E. coli in LB medium. For purification of low-copy plasmids and cosmids, large plasmids (>10 kb), *and DNA prepared using other methods,*

Procedure

1. **Resuspend pelleted bacterial cells in 250 µl Buffer P1 and transfer to a microcentrifuge tube**. Ensure that RNase A has been added to Buffer P1. No cell clumps should be visible after resuspension of the pellet. If LyseBlue reagent has been added to Buffer P1, vigorously shake the buffer bottle to ensure LyseBlue particles are completely dissolved. The bacteria should be resuspended completely by vortexing or pipetting up and down until no cell clumps remain.
2. **Add 250 µl Buffer P2 and mix thoroughly by inverting the tube 4–6 times**. Mix gently by inverting the tube. Do not vortex, as this will result in shearing of genomic DNA. If necessary, continue inverting the tube until the solution becomes viscous and slightly clear. Do not allow the lysis reaction to proceed for more than 5 min. If LyseBlue has been added to Buffer P1 the cell suspension will turn blue after addition of Buffer P2. Mixing should result in a homogeneously colored suspension. If the suspension contains localized colorless regions or if brownish cell clumps are still visible, continue mixing the solution until a homogeneously colored suspension is achieved.7
3. **Add 350 µl Buffer N3 and mix immediately and thoroughly by inverting the tube 4–6 times**. To avoid localized precipitation, mix the solution thoroughly, immediately after addition of Buffer N3. Large culture volumes (e.g. ≥ 5 ml) may require inverting up to 10 times. The solution should become cloudy. If LyseBlue reagent has been used, the suspension should be mixed until all trace of blue has gone and the suspension is colorless. A homogeneous colorless suspension indicates that the SDS has been effectively precipitated.
4. **Centrifuge for 10 min at 13,000 rpm (~17,900 x g) in a table-top microcentrifuge**. A compact white pellet will form.
5. **Apply 800 µl of the supernatant from step 4 to the QIAprep 2.0 spin column by pipetting.**
6. **Centrifuge for 30–60 s. Discard the flow-through.**
7. **Recommended: Wash the QIAprep 2.0 spin column by adding 0.5 ml Buffer PB and centrifuging for 30–60 s. Discard the flow-through**.
   This step is necessary to remove trace nuclease activity when using endA+ strains such as the JM series, HB101 and its derivatives, or any wild-type strain, which have high levels of

nuclease activity or high carbohydrate content. Host strains such as XL-1 Blue and DH5®α do not require this additional wash step.

8. **Wash QIAprep 2.0 spin column by adding 0.75 ml Buffer PE and centrifuging for 30–60 s**.
9. **Discard the flow-through, and centrifuge at full speed for an additional 1 min to remove residual wash buffer**.

   Important: Residual wash buffer will not be completely removed unless the flow-through is discarded before this additional centrifugation. Residual ethanol from Buffer PE may inhibit subsequent enzymatic reactions.
10. **Place the QIAprep 2.0 column in a clean 1.5 ml microcentrifuge tube. To elute DNA, add 50 µl Buffer EB (10 mM Tris·Cl, pH 8.5) or water to the center of each QIAprep 2.0 spin column, let stand for 1 min, and centrifuge for 1 min.**

7.2 Western Blot (WB)

The WB is a widely used analytical technique to detect specific proteins in a sample of tissue homogenate or extract. Protein samples (nearly 100 ng) were prepared with loading buffer and subject to SDS-PAGE. Gel electrophoresis was carried out at 100V for 2.5 h to separate the denatured protein by polypeptide size. Then, the protein samples were transferred onto a nitrocellulose membrane (Bio-Rad). The membrane was blocked by 5% (w/v) milk dissolved in tris buffered saline (TBS) for 1 h to avoid any nonspecific binding of antibodies on the surface of the membrane. Then, the membrane was incubated for 1 h with a primary antibody which could specifically bind to the proteins and subsequently with a secondary antibody which binds the primary antibody (**Error! Reference source not found.**). The membrane was washed with tween tris buffered saline (TTBS) buffer for 3 times before each antibody incubation and every wash lasted for 10 min to remove the unbound antibody. Considering the protein samples, we used different primary antibodies, shown in detail in Table 3.3. All antibodies were dissolved in TBS buffer, stored at 4°C and used for several times. 60 Horseradish peroxidase (HRP) conjugated to the secondary antibody is an enzyme frequently used as an indicator in WB. A substrate named Super-Signal West Pico Chemiluminescent Substrate (Thermo Fisher Scientific) reacts with HRP and produces a signal which is detected on the Medical X-ray film (AGFA) in an electrophoresis systems autoradiography cassette.

Table 7-1 - WB samples and antibodies used

Sample	Lactonase
Source and expression	BL21
Primary antibody	sab1305538-40tst
Primary antibody dilution	1/1000
Secondary antibody	Goat anti-mouse IgG-HRP
Secondary antibody dilution	1/5000

7.3 SDS-PAGE and Coomassie blue staining

SDS-PAGE is used to separate proteins from a mixture according to their size. SDS-PAGE system was composed of a separating gel (bottom) and a stacking gel (upper) which were prepared using the reagents listed in Table 3.1. Separating gel was added to the glass slot and of isopropanol was used to flat and seal up the surface. Once the separating gel was solidified, isopropanol was removed and the stacking gel was prepared. A comb was inserted to form the lanes. Proteins were prepared and mixed with 4x protein loading buffer and loaded onto the gel. The gel was run in the 1x TGS buffer for 2.5 h at 100V. After electrophoresis, the gel was stained with Coomassie brilliant blue buffer for 3 h and destained with Coomassie destain buffer until the protein bands were visible.

Table 7-2 SDS-PAGE preparation

	Separating Gel		Stacking Gel	
Components (stock)	Final Concentration	10ml	Final Concentration	5ml
Acr/Bis (37.5%)	12%	3.2ml	5%	0.67ml
Tris-HCl (1.5M pH 8.8)	0.75M	5ml	---	---
Tris-HCl (0.5M pH 6.8)	---	---	0.125M	1.25ml
SDS (10%)	0.10%	0.1ml	0.10%	0.05ml
APS	0.10%	0.1ml	0.10%	0.05ml
TEMED	0.50%	0.05ml	0.50%	0.025ml
ddH20		1.55ml		2.955ml